HB-EGF-loaded nanovesicles enhance trophectodermal spheroid attachment and invasion

Qi Hui Poh[1], alin rai[1], Jonathon Cross[1], and David Greening[1]

[1]Baker Heart and Diabetes Institute

August 24, 2023

Abstract

The ability of trophectodermal cells (outer layer of the embryo) to attach to the endometrial cells and subsequently invade the underlying matrix are critical stages of embryo implantation during successful pregnancy establishment. Extracellular vesicles (EVs) have been implicated in embryo-maternal crosstalk, capable of reprogramming endometrial cells towards a pro-implantation signature and phenotype. However, challenges associated with EV yield and direct loading of biomolecules limit their therapeutic potential. We have previously established generation of cell-derived nanovesicles (NVs) from human trophectodermal cells (hTSCs) and their capacity to reprogram endometrial cells to enhance adhesion and blastocyst outgrowth. Here, we employed a rapid NV loading strategy to encapsulate potent implantation molecules such as HB-EGF (NVHBEGF). We show these loaded NVs elicit EGFR-mediated effects in recipient endometrial cells, activating kinase phosphorylation sites that modulate their activity (AKT S124/129, MAPK1 T185/Y187), and downstream signalling pathways and processes (AKT signal transduction, GTPase activity). Importantly, they enhanced target cell attachment and invasion. The phosphoproteomics and proteomics approach highlight NVHBEGF-mediated short-term signalling patterns and long-term reprogramming capabilities on endometrial cells which functionally enhance trophectodermal-endometrial interactions. This proof-of-concept study demonstrate feasibility in enhancing the potency of NVs in the context of embryo attachment and establishment.

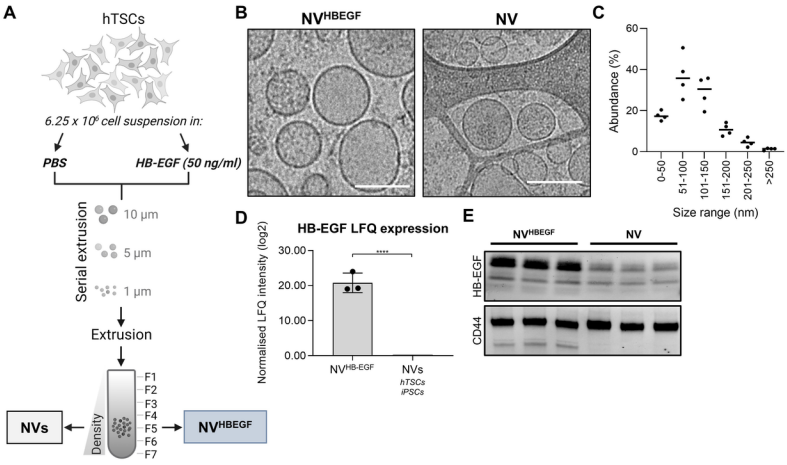

Figure 1. Production and characterisation of NV$^{HB\text{-}EGF}$

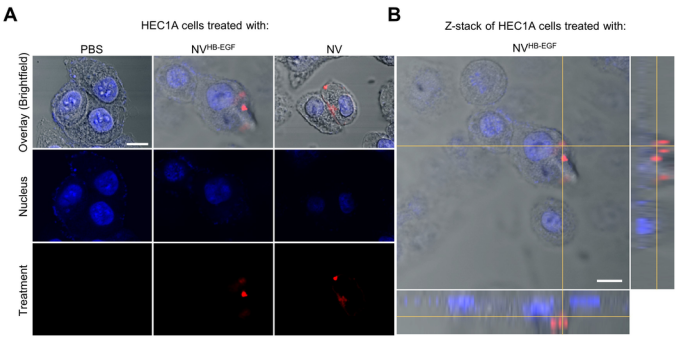

Figure 2. Uptake of $NV^{HB\text{-}EGF}$ and NVs by endometrial HEC1A cells

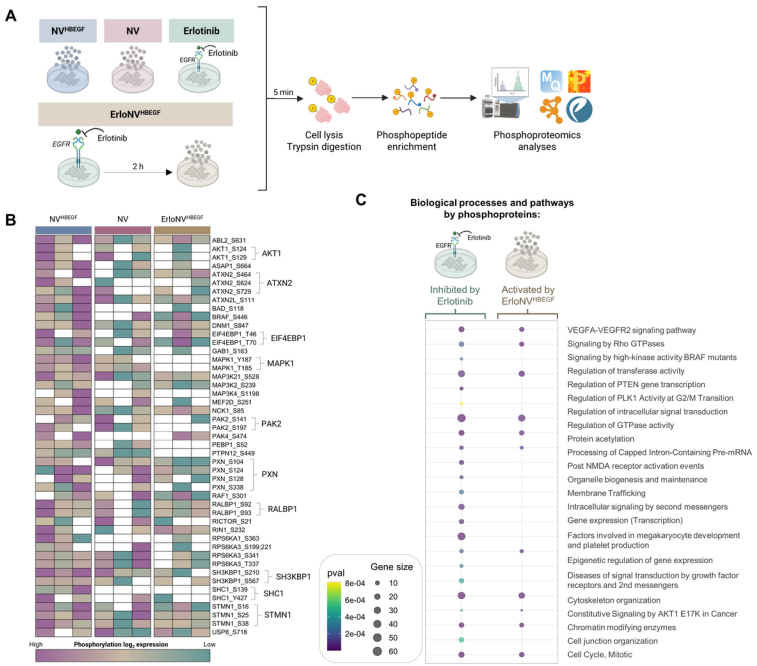

Figure 3. NV^{HBEGF} remodel the phosphoproteome landscape in HEC1A endometrial cells

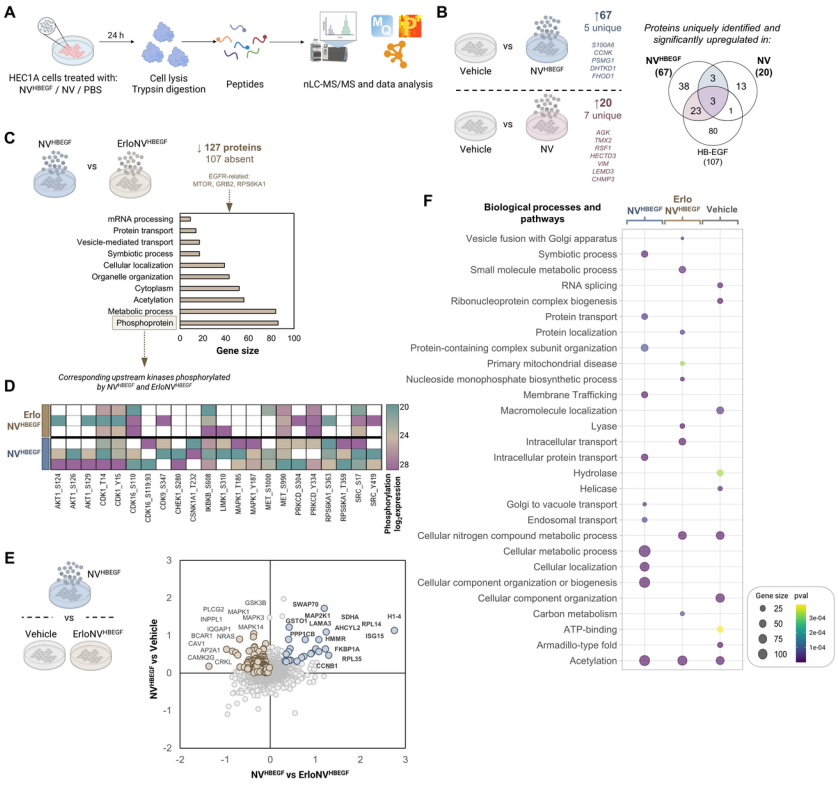

Figure 4. NV^{HBEGF} remodel the proteome landscape and EGFR signaling network at the time of implantation

HB-EGF-loaded nanovesicles enhance trophectodermal spheroid attachment and invasion

Qi Hui Poh[1,2,3], Alin Rai[1,3,4], Jonathon Cross[1], David W Greening[1,3,4,5*]

[1]Baker Heart and Diabetes Institute, Molecular Proteomics, Melbourne, Victoria, Australia. [2]Department of Biochemistry and Chemistry, School of Agriculture, Biomedicine and Environment, La Trobe University, Bundoora, Victoria, Australia. [3]Department of Cardiovascular Research, Translation and Implementation, La Trobe University, Melbourne, Victoria, Australia. [4]Central Clinical School, Monash University, Melbourne, Victoria, Australia. [5]Baker Department of Cardiometabolic Health, University of Melbourne, Melbourne, Victoria, Australia.

*To whom correspondence should be addressed:
David W. Greening
Molecular Proteomics, Baker Heart and Diabetes Institute
75 Commercial Road, Melbourne, 3004, Australia
Email: David.Greening@baker.edu.au

ORCID
Qi Hui Poh – 0000-0003-2620-2834; Alin Rai – 0000-0001-7994-5151; Jonathon Cross – 0009-0006-3057-8964; David W Greening – 0000-0001-7516-485X

Keywords
Nanovesicles, proteomics, phosphorylation, signalling, embryo-endometrial crosstalk

Abstract

The ability of trophectodermal cells (outer layer of the embryo) to attach to the endometrial cells and subsequently invade the underlying matrix are critical stages of embryo implantation during successful pregnancy establishment. Extracellular vesicles (EVs) have been implicated in embryo-maternal crosstalk, capable of reprogramming endometrial cells towards a pro-implantation signature and phenotype. However, challenges associated with EV yield and direct loading of biomolecules limit their therapeutic potential. We have previously established generation of cell-derived nanovesicles (NVs) from human trophectodermal cells (hTSCs) and their capacity to reprogram endometrial cells to enhance adhesion and blastocyst outgrowth. Here, we employed a rapid NV loading strategy to encapsulate potent implantation molecules such as HB-EGF (NV^{HBEGF}). We show these loaded NVs elicit EGFR-mediated effects in recipient endometrial cells, activating kinase phosphorylation sites that modulate their activity (AKT S124/129, MAPK1 T185/Y187), and downstream signalling pathways and processes (AKT signal transduction, GTPase activity). Importantly, they enhanced target cell attachment and invasion. The phosphoproteomics and proteomics approach highlight NV^{HBEGF}-mediated short-term signalling patterns and long-term reprogramming capabilities on endometrial cells which functionally enhance trophectodermal-endometrial interactions. This proof-of-concept study demonstrates feasibility in enhancing the functional potency of NVs in the context of embryo implantation.

Significance statement

Nanosized extracellular vesicles and a plethora of growth factors (i.e., HB-EGF) are critical signalling mediators during embryo implantation to the maternal endometrium – a cardinal event of pregnancy establishment. This study highlights a rapid and scalable cell extrusion method to load HB-EGF into trophectodermal cell-derived nanovesicles (NV^{HBEGF}). We report, through phosphoproteomics and proteomics analyses, NV^{HBEGF} short-term signalling and long-term reprogramming capabilities on recipient endometrial cells, including but not limited to EGFR-mediated phosphorylation patterns, downstream signalling events, and cellular processes intimately associated with embryo implantation and endometrial receptivity. Importantly, the application of NV^{HBEGF} stimulated heightened endometrial-trophectodermal attachment, and trophectodermal invasion – pivotal events in the early stages of pregnancy. We have thus harnessed trophectodermal NVs loaded with HB-EGF to orchestrate multifaceted signalling and cellular events in endometrial cells crucial for pregnancy establishment. Loaded NVs possess immense potential for therapeutic development and warrants further investigation.

Introduction

Embryo implantation is a multi-step process comprising blastocyst apposition and attachment to the maternal endometrial epithelium by its outer trophectodermal layer and its subsequent invasion into the underlying tissue for intrauterine development[1-3]. Its failure accounts for ~75% of unsuccessful pregnancy outcomes in Assisted Reproductive Technologies (ART)[1-3], presenting a significant hurdle for human reproduction. Paramount for successful implantation, reciprocal embryo-maternal communication[4, 5] mediated by secreted signalling players[6-8] such as hormones (hCG[9]), cytokines (LIF[10], IL-18[11]), and growth factors (GM-CSF[12], G-CSF[13]) remains an ongoing topic of investigation in reproductive biology, with efforts to develop them as diagnostic markers of uterine receptivity or therapeutic supplements to enhance implantation success, extending into clinical trials.

Of increasing interest as a signalling modality are extracellular vesicles (EVs)[14, 15]; membrane-bound nanosized (30-1000 nm) vesicles that transport and deliver bioactive lipids, proteins, and genetic material to recipient cells, reprogramming and altering their molecular signature and phenotype[16-19]. Indeed, EVs from human embryos and trophectodermal cells (hTSCs) harbour critical regulators of implantation that reprogram recipient endometrial proteome to enhance embryo-endometrial attachment[17]. However, their isolation procedures are tedious and time-consuming, prompting investigation into an EV-like alternative; nanovesicles (NVs), generated by serial extrusion of parental cells[20-23]. From hTSCs, NVs displayed similar biophysical and functional properties to EVs, significantly promoting trophectoderm-endometrial attachment and embryo outgrowth (*Proteomics, in review*). As extrusion is recognised as an effective approach for drug loading into nanocarriers such as EVs and liposomes (4-fold higher than passive methods)[24], this methodology enables opportunities for NV cargo modification. Indeed, loaded EVs and NVs are increasingly explored as fertility therapeutics[25, 26]. For example, human chorionic gonadotropin (hCG), a potent embryonic signal, was loaded into uterine fluid EVs (UF-EV^{hCG}) and treated onto endometrial cells, enhancing their expression of receptivity markers[26]. Similarly, enrichment of NVs with known regulators of implantation may enhance or confer specific functions while retaining certain influential characteristics of parental cells, such as surface-expressed molecules that facilitate interaction with target recipient cells[20, 27], or natural composition of bioactive molecules that contribute to desired functional outcomes[22, 23, 28].

Amongst the molecules investigated for facilitating embryo-maternal crosstalk that governs successful implantation, heparin-binding EGF-like growth factor (HB-EGF)[29-33] remains one of the longest-standing and well-established. With potent embryotropic and endometrial reprogramming capabilities, HB-EGF is secreted by both the developing blastocyst and the receptive endometrium; importantly, both entities express its cognate receptors[34], and are thus responsive to its role in mediating surface interactions, and downstream signalling cascades. Indeed, EGFR, MAPK, and PI3K-AKT signalling

pathways and their associated processes are indispensable for successful embryo and endometrial reprogramming[35-37] during implantation and throughout pregnancy. In this study, we employed the extrusion methodology to enrich hTSC NVs with HB-EGF (NV^{HBEGF}) and investigated the response of low-receptive HEC1A endometrial recipient cells at a molecular level, including protein phosphorylation changes and global proteome reprogramming. Further, we assessed NV^{HBEGF} functional capacity to enhance trophectodermal spheroid attachment on stimulated endometrial cells and trophectodermal spheroid invasion into Matrigel™.

Materials and methods

Cell culture

Human trophectodermal cells (T3-TSC) (kind gift from Prof. Susan Fisher, UCSF) were derived from individual blastomeres of donated human embryos.[38] Cells were grown as a monolayer and routinely maintained as described[39] in DMEM/F12 (Gibco, Invitrogen) supplemented with 1% v/v Penicillin-Streptomycin (P/S) and 10% v/v foetal calf serum (FCS, Gibco, Invitrogen), with addition of 10 ng/ml bovine fibroblast growth factor (bFGF, R&D Systems) and 10 µM SB431542 (#1614, Tocris Bioscience) to maintain a trophectoderm-like state. Cells were grown on flasks coated with 0.5% gelatin prior to experimental seeding and passaged using Trypsin-EDTA (Gibco). Spheroids were generated as described[39, 40] with slight modifications. T3-TSC cells were seeded at 1500 cells per well in an ultra-low adhesion round-bottom 96-well plate in 100 µl of trophectoderm medium and incubated for 72 h.

HEC1A endometrial epithelial cells

Human endometrial carcinoma HEC1A cells (HTB-112) were a kind gift from Professor Lois Salamonsen purchased from American Type Culture Collection (ATCC; Rockville, MD). Endometrial cells were routinely maintained in DMEM/F12 supplemented with 1% P/S, and 5% v/v FCS and incubated at 37°C with 5% CO_2. Cells were routinely passaged using 0.5% v/v trypsin-EDTA (Gibco). Prior to treatments used in this study, cells were cultured in basal media overnight comprising DMEM/F12 supplemented with 0.6% insulin transferrin selenium (ITS, Gibco) and 1% v/v P/S.

Generation of hTSC NVs and loaded NV^{HBEGF}

NV^{HBEGF} generation and purification were performed as described[20, 21, 28] with modifications (N=3). Briefly, T3-TSC human trophectodermal cells (approximately 6.25 x 10^6 cells per T-75 flask) were rinsed twice with PBS and detached with 10 mM EDTA (Sigma-Aldrich). The cell suspension was pelleted at 500 g for 5 min and re-suspended in ice-cold PBS containing 50 ng/ml human recombination human epidermal-like growth factor (HB-EGF) (#4266-50, Abcam). The cell suspension was sequentially extruded through 10, 5, and 1 µm pore-sized polycarbonate membranes (Nuclepore,

Whatman Inc., Clifton, NJ, USA) thirteen times across each filter using a mini extruder system (Avanti Polar Lipids, Birmingham, AL, USA). For unloaded NVs, the cell pellet was re-suspended in ice-cold PBS prior to sequential extrusion. Extruded NV^{HBEGF} and NVs were subsequently isolated using 10% OptiPrep™ (Stemcell Technologies) density cushion (step gradient formed by overlaying extruded sample on 10% and 50% iodixanol) and centrifuged at 100 000 g for 2 h at 4°C. Seven equal fractions were collected, diluted in PBS (to 1.5 ml), and ultracentrifuged at 100 000 g for 1 h at 4°C (TLA-55 rotor; Optima MAX-TL ultracentrifuge). NV^{HBEGF} and NVs pellets were resuspended in PBS and stored in 1 µg/ul aliquots at −80°C until use.

Co-culture attachment assay

HEC1A endometrial epithelial cells were used to model a low-receptive endometrium[41-44]. HEC1A cells were seeded at confluency onto round-bottom 96-well plates before overnight culture in basal media (DMEM/F12 supplemented with 1% v/v P/S), followed by a 24-h treatment with NV^{HBEGF} or NVs (50 µg/ml), HB-EGF (50 ng/ml), PBS (volume matched), Erlotinib (20 nM), or sequential Erlotinib (20 nM) for 2 h followed by NV^{HBEGF}. T3-TSC spheroids (1500 cells per spheroid, 1 spheroid per well) were transferred to stimulated endometrial cells and allowed to attach for 1 h, after which the media was aspirated and washed gently once with PBS. Spheroid adhesion (%) for each treatment was calculated by: [(number of attached spheroids/number of seeded spheroids) x 100] (n=12, N=5).

hTSC spheroid Matrigel invasion assay

hTSC spheroid invasion assays were performed with growth factor reduced Matrigel™ matrix (Corning) as previously described[45]. Briefly, hTSC spheroids were suspended in 100 µl DMEM/F-12 media containing 1% (v/v) Pen/Strep, 0.1% ITS, and either NV^{HBEGF} or NVs (50 µg/ml), HB-EGF (50 ng/ml), PBS (volume matched), Erlotinib (20 nM), or sequential Erlotinib (20 nM) for 2 h followed by NV^{HBEGF} ($ErloNV^{HBEGF}$). The spheroid suspension (2-3/well) was overlaid onto Matrigel™ in 8-well microscopy chambers (Corning) and incubated for 24 h at 37°C. Subsequently, 50 µl media was removed from each well, mixed 1:1 with Matrigel™, then gently overlaid back onto the spheroids. Matrigel™ was then allowed to solidify for 30 min at 37°C prior to adding 200 µl of DMEM/F-12 [10% (v/v) FBS, 1% (v/v) Pen/Strep] containing the treatments as above. After 72 h, spheroids were imaged using Olympus FSX100. The extent of invasion (% increase) was quantified using ImageJ and calculated by: [(outer—inner circumference)/(inner circumference) × 100]. Data presented as a box plot was generated from individual points ($n \geq 8$) per treatment, providing the interquartile range and minimum, median, and maximum values of each treatment.

Protein quantification and western blotting

All samples were lysed in 1% v/v sodium dodecyl sulphate (SDS), 50 mM triethylammonium bicarbonate (TEAB), pH 8.0, incubated at 95 °C for 5 mins and quantified by microBCA assay (Thermo

Fisher Scientific) as described[46]. Western blot sample buffer (4% w/v SDS, 20% v/v glycerol, and 0.01% v/v bromophenol blue, 0.125 M Tris-hydrochloride (Tris-HCl), pH 6.8) was added in a 1:1 v/v ratio to lysed samples with 100 mM dithiothreitol (DTT, Thermo Fisher Scientific). Samples (10–20 µg) were resolved on Norvex 4–12% Bis–Tris NuPAGE gels with MES running buffer at 150 V for 1 h. Proteins on the gel were electrotransferred onto nitrocellulose membranes using iBlot™ Dry 2.0 blotting system (Life Technologies) at 12 V for 8 min. The membranes were blocked with 5% w/v skim milk powder in PBS-Tween (PBST) (0.137 M NaCl, 0.0027 M KCl, 0.01 M Na_2HPO_4, 0.0018 M KH_2PO, 0.05% w/v Tween 20) for 30 min at room temperature. The membranes were washed and probed with primary antibodies (1:1000 dilution) for 24 h at 4 °C in PBST. Primary antibodies used include mouse monoclonal against CD44 (#119863, Abcam), and HB-EGF (#27450, Cell Signaling Technology). Secondary antibodies used were: IRDye 800 goat anti-mouse IgG (#926-32210) or IRDye 680 goat anti-rabbit IgG (#926-68071) (1:15000, LI-COR Biosciences).

Biophysical particle analysis

Cryo-electron microscopy imaging (Tecnai G2 F30) of NV^{HBEGF} and NVs was performed as described[47]. Briefly, NVs (~1 µg protein) were transferred onto glow-discharged C-flat holey carbon grids (ProSciTech Pty Ltd., Kirwan, Australia). Excess liquid was blotted, and grids were frozen in liquid ethane. Grids were mounted in a Gatan cryoholder (Gatan, Inc.,Warrendale, PA, USA) in liquid nitrogen. Images were acquired at 300 kV using a Tecnai G2 F30 (FEI, Eidhoven, The Netherlands) in low dose mode.

Lipophilic dye labelling and uptake assay

For NV staining (NV^{HBEGF} and NV), NVs were incubated with Vybrant™ DiI Cell-Labeling Solution at 1:200 dilution (Invitrogen, V22885) at 1 µM concentration for 15 min at 37°C as described[48]. Unbound dye was removed by subjecting labelled NVs (volume-matched DiI-PBS as label control) to centrifugation at 100 000 g (1 h) on a 10% OptiPrep™ cushion. Pelleted DiI-NVs were resuspended in 50 µl of PBS. HEC1A cells grown to 70% confluency in 8-well glass chamber slide (Sarstedt) were incubated with DiI-labelled NVs at 37°C for 2 h, then washed twice with PBS. Nuclei were stained with Hoechst stain (10 µg/ml) for 10 min and fixed using 4% formaldehyde for 5 min and imaged with Nikon A1R confocal microscope equipped with resonant scanner, using a 20x WI (1.2 NA); (Nikon, Tokyo, Japan). Images were sequentially acquired. The XY image resolution was 1024 x 1024 at 0.033 FPS, 4x averaging, 2.4 dwell time. 3D images were taken by Z-stack of approximately 15 µm, 25 steps, at a resolution of 1024 x 1024, 8x averaging 2.4 dwell time. NS studio was used to render images.

Proteomics: solid-phase-enhanced sample preparation

All samples, including NV^{HBEGF} and NVs (n=3), stimulated HEC1A cells for phosphoproteomics (n=3) and global proteomics (n=4) were lysed in 1% v/v sodium dodecyl sulphate (SDS), 50 mM

triethylammonium bicarbonate (TEAB), pH 8.0, incubated at 95 °C for 5 mins and quantified by microBCA (Thermo Fisher Scientific) as described[46]. Proteomic sample preparation using single-pot solid-phase-enhanced sample preparation (SP3)[49] was performed on protein extracts (10 µg, 300 µg for phosphoproteomics) as previously described[17]. Briefly, samples were reduced with 10 mM DTT at RT for 1 h (350 rpm), alkylated with 20 mM iodoacetamide (IAA) (Sigma-Aldrich) for 20 min at RT (light protected), and quenched with 10 mM DTT. A Sera-Mag SpeedBead carboxylate-modified magnetic particle mixture (1:1 hydrophilic and hydrophobic mix, 65152105050250, 45152105050250, Cytiva) was added to protein extracts and incubated in 50% v/v ethanol for 10 min (1000 rpm) at RT. Beads were sedimented on a magnetic rack to remove the supernatant. Beads were washed three times with 200 µL 80% v/v ethanol, then resuspended in 100 µL 50 mM TEAB pH 8.0 and digested overnight with trypsin (1:50 trypsin: protein ratio; Promega, V5111) at 37 °C, 1000 rpm. The peptide and bead mixture were centrifuged at 20,000 g for 1 min at RT. Samples were then placed on a magnetic rack and the supernatant was collected, acidified to a final concentration of 1.5% formic acid, frozen at -80 °C for 20 min, and dried by vacuum centrifugation. Peptides were resuspended in 0.07% trifluoroacetic acid (TFA), quantified by Fluorometric Peptide Assay (Thermo Fisher Scientific, 23290) as per manufacturer's instructions, and normalised to 0.5 µg/µl with 0.07% TFA.

Phosphopeptide enrichment

Peptide digests from each HEC1A cell treatment group (n=3) were lyophilised by vacuum centrifugation and reconstituted in Binding/Equilibration Buffer for phosphopeptide enrichment[45] using High-Select™ TiO_2 Phosphopeptide Enrichment kit (Thermo Fisher Scientific, A32993), as per manufacturer's instructions. Briefly, peptide digests were transferred to a pre-equilibrated TiO_2 spin tip and centrifuged twice at 1000 g, 5 min. The column was washed twice with binding/equilibration buffer and subsequent wash buffer at 3000 g, 2 min, then with MS-grade water at 3000 g, 2 min. Phosphopeptides were eluted in 100 µl phosphopeptide elution buffer by centrifugation at 1000 g, 5 min, dried by vacuum centrifugation, and reconstituted in 0.07% TFA before quantification by Colorimetric Peptide Assay (ThermoFisher Scientific, #23275) as per manufacturer's instructions.

Liquid Chromatography–Tandem Mass Spectrometry

Peptides were analysed on a Dionex UltiMate NCS-3500RS nanoUHPLC coupled to a Q-Exactive HF-X hybrid quadrupole-Orbitrap mass spectrometer equipped with a nanospray ion source in positive, data-dependent acquisition mode as described[50]. Peptides were loaded (Acclaim PepMap100 C18 5 µm beads with 100 Å pore-size, Thermo Fisher Scientific) and separated (1.9-µm particle size C18, 0.075 × 250 mm, Nikkyo Technos Co. Ltd) with a gradient of 2–80% acetonitrile containing 0.1% formic acid over 110 min at 300 nL min-1 at 55°C (in-house enclosed column heater). An MS1 scan was acquired from 350–1,650 m/z (60,000 resolution, 3×10^6 automatic gain control (AGC), 128 msec injection time) followed by MS/MS data-dependent acquisition (top 25) with collision-induced

dissociation and detection in the ion trap (30,000 resolution, 1×10^5 AGC, 60 msec injection time, 28% normalized collision energy, 1.3 m/z quadrupole isolation width). Unassigned precursor ions charge states and slightly charged species were rejected and peptide match disabled. Selected sequenced ions were dynamically excluded for 30 sec. The mass spectrometry-based proteomics data is deposited to the ProteomeXchange Consortium via the MASSive partner repository and available via MASSive with the identifier MSV000092562.

Data Processing and Bioinformatics

Peptide identification and quantification were performed as described previously[39, 50] using MaxQuant (v1.6.14) with its built-in search engine Andromeda[51]. Tandem mass spectra were searched against *Homo sapiens* (human) reference proteome (74,811 entries, downloaded 12-2019) supplemented with common contaminants. Search parameters included carbamidomethylated cysteine as fixed modification and oxidation of methionine and N-terminal protein acetylation as variable modifications. Data was processed using trypsin/P as the proteolytic enzyme with up to 2 missed cleavage sites allowed. The search tolerance and fragment ion mass tolerance were set to 7 ppm and 0.5 Da, respectively, at less than 1% false discovery rate on peptide spectrum match (PSM) level employing a target-decoy approach at peptide and protein levels. Protein group or phosphorylation site tables were imported into Perseus (v1.6.7) for analysis, with contaminants and reverse peptides removed. Label free quantification (LFQ) algorithm in MaxQuant was used to obtain quantification intensity values and processed using Perseus as described[52]. Cytoscape[53] (v3.9.1) with STRING and EnrichmentMap plugins were used for functional enrichment analyses (KEGG, Reactome, Gene Ontology (GO) biological process) of proteins and to generate protein-protein interaction networks. The kinase-substrate database from PhosphoSite Plus was used to identify upstream kinases for phosphorylated proteins.

Statistical Analysis

Data clean up and analysis were performed using Perseus (MaxQuant computational platform) and Excel. Protein intensities were $\log_2$ transformed and subjected to one-way ANOVA followed by Post hoc Tukey's HSD test to identify significant differences between treatment groups. For stimulated HEC1A endometrial cells, proteins identified in ≥2 replicates (out of 3) or ≥3 replicates (out of 4) in each group were included in analysis. Phosphorylated sites (phosphosites) with a localisation probability of >75% and quantified in ≥2 out of 3 replicates per treatment group were included in the analysis. GraphPad Prism v9.4.1 and R (2022.02.3+492) were used for statistical analysis of functional data. One-way ANOVA for multiple comparisons or unpaired t-test was performed. All data is presented as mean plus/minus standard deviation (mean±SD). P-value<0.05 is considered statistically significant.

Results

3.1. Generation of HB-EGF-loaded NVs (NV^{HBEGF}) from human trophectodermal cells (hTSCs)

Cell-derived NVs were generated by serial extrusion of hTSCs (6.25×10^6) suspended in PBS through microfilters of decreasing pore size (10-5-1 μm) as described[28]. To generate NVs loaded with HB-EGF (NV^{HBEGF}), we serially extruded hTSCs in PBS containing 50 ng/ml of HB-EGF (**Figure 1A**). NVs were then isolated using density gradient separation[28] (**Figure 1A**). NVs and NV^{HBEGF} displayed similar buoyant densities of 1.10-1.20 g/cm^3, and cryo electron microscopy revealed that NVs were spherical in shape and morphologically intact (**Figure 1B**), ranging 20-250 nm in diameter (mean 104.2 nm) (**Figure 1C**), consistent with NVs[28] generated previously. We next questioned whether HB-EGF is successfully incorporated into NVs. We subjected NVs (NVs and NV^{HBEGF}, n=3) to mass spectrometry-based proteomic profiling (**Figure 1D**). Based on stringent peptide and protein identification criteria we quantified HB-EGF in all NV^{HBEGF} biological replicates, compared to unloaded NVs. We orthogonally validated loading of HB-EGF into NVs using a monoclonal antibody specific to human HB-EGF protein by Western blotting (**Figure 1E**).

3.2. NV^{HBEGF} uptake by recipient endometrial HEC1A cells

Previously, we have shown that hTSC NVs can be taken up by endometrial HEC1A cells to enhance their attachment to hTSC cell spheroids (*in review, Proteomics*). Here, we questioned whether loading of HB-EGF into NVs impacts their uptake. For this, NV^{HBEGF} were labelled with fluorescent lipophilic DiI dye (red) and incubated with HEC1A cells over a 2-hr period. Confocal fluorescence microscopy revealed that NV^{HBEGF}, similar to unloaded NVs, were readily taken up by HEC1A cells (**Figure 2A**). Imaging along the z-axis showed that NV^{HBEGF} were internalised and appeared as punctuate structures, typical of vesicle uptake by recipient cells[17, 45] (**Figure 2B)**.

3.3. NV^{HBEGF}-mediated phosphorylation is linked to intracellular signal transduction and EGFR signalling

HB-EGF activates various receptors (e.g., PRLR[54], CD44[55, 56]) but their effect on receptor tyrosine kinases (RTKs)[57] ERBB2/4 and especially EGFR, are more prominently studied. HB-EGF activation of EGFR[58] induce receptor conformation changes, internalisation, and intracellular localisation; and downstream activation of the RAS-RAF-MEK-ERK, PI3K-AKT, STAT, and NF-kappa-B signalling pathways[58] which have roles in modulating cell adhesion and motility. However, phosphorylation patterns, signalling dynamics, and functional outcomes downstream of EGFR activation remain poorly understood[59]. For insights into whether the HB-EGF loaded into NVs are functional in recipient

HEC1A cells, we stimulated HEC1A cells with NV^{HBEGF} and NVs (5 min treatment) and performed phosphoproteomics analysis (**Figure 3A, Table S1**). Further, to investigate the dynamic cellular signalling events initiated by NV^{HBEGF}; Erlotinib[58], an EGFR inhibitor; was used as a pre-treatment to suppress NV^{HBEGF}-mediated EGFR signalling in HEC1A cells ($ErloNV^{HBEGF}$) (**Figure 3A**).

NV^{HBEGF} treatment, compared to NVs, resulted in unique phosphorylation of 303 proteins and identification of 396 phosphopeptide sites in HEC1A cells, including EGFR signalling regulators ERRFI1 S273[60], PRKCD S304[61], RALBP1 S99, RICTOR S21[62], and SHC1 S139[63] (**Table S2**). Following treatment on target cells, NV^{HBEGF} also upregulated ($log_2fc \geq 0.5$) 705 phosphoproteins and 1218 phosphopeptide sites compared to NV, include those downstream of EGFR activation (**Figure 3B, Figure S1, Table S2**). However, Erlotinib pre-treatment attenuated phosphorylation of SH3KBP1 S210 and AKT1 S124[64] and S129[65], potentially limiting its response to activation and kinase activity. Additionally, phosphorylation of MAPK1 T185 and Y187 (mediated by EGFR[66]) were not detected, along with MAP3K4 S1198, PEBP1 S52, and PTPN12 S449 (**Figure 3B and S1, Table S2**); indicative of NV^{HBEGF}-mediated activation of EGFR signalling in HEC1A cells. Interestingly, Erlotinib also reduced expression of phosphorylated proteins associated with endometrial receptivity[67, 68] (MAPK1, ANK3, GPRC5C, KIF4A, NDRG1, BAG3, FMNL2, KANK2, LNPK, LIMCH1, MVB12A, NAB2, TBC1D1, UIMC1) and embryo implantation[68] (PEBP1, CARMIL1, PHLDB2, EPB41L1, REPS1, NDRG1, SCML2, SEMA6A, SHROOM2, STX, WWC1), which were upregulated by NV^{HBEGF} compared to NVs (**Figure 3B, Table S2**). Inhibition of EGFR-mediated signalling may thus result in altered expression and activation of proteins/phosphoproteins critical for endometrial function.

For insights into the downstream cellular processes and signalling pathways affected by EGFR inhibition following NV treatment, we performed functional enrichment analysis on 421 proteins which phosphorylation were inhibited by Erlotinib (**Table S3**). From this subset of proteins, we identify various networks enriched including intracellular signalling, gene expression, cytoskeleton organisation, and AKT1, BRAF and GTPase activity – processes downstream of EGFR activation, were amongst those downregulated (**Figure 3C**). Subsequent NV^{HBEGF} treatment induced phosphorylation of 261 out of 421 Erlotinib-inhibited proteins, which are associated with GTPase activity, AKT1 and intracellular signal transduction, and the VEGF-VEGFR2 signalling pathway (**Figure 3C**, **Table S4**), indicative of an alternative signalling mechanism to EGFR activation.

From this profiling analysis we demonstrate that NVs loaded with HB-EGF can mediate rapid (5 min) and dynamic changes in the phosphorylation landscape of HEC1A endometrial cells, including regulators of intracellular signal transduction and EGFR signalling networks, as well as known regulators of endometrial receptivity.

3.4. NV^{HBEGF} treatment on recipient HEC1A endometrial cells significantly increased expression of proteins upregulated at the embryo-maternal interface

Embryo implantation into the maternal endometrium takes approximately 1 to 2 days[69]. To define the influence of earlier NV^{HBEGF}-mediated phosphorylation and signalling events on endometrial cell proteome at the time of implantation, we investigated the proteome landscape of HEC1A endometrial cells following 24 hr stimulation with NV^{HBEGF}, NVs, HB-EGF, ErloNV^{HBEGF}, or PBS (vehicle) **(Figure 4A, Table S5)**. Compared to vehicle, 67 proteins were uniquely identified and significantly upregulated following NV^{HBEGF} treatment (**Figure 4B**), including proteins present either at the embryo-maternal interface[68, 70] (S100A16/6/4[71], TAGLN2[72-74], PTGFRN[75], CKAP4, TPD52L2, UFL1, NDUFB10, GALNT2, RAPH1), in the endometrium during pre-attachment (CSTB[76]), or associated with placental development (FTL[77], LAMP1[78-80], LRP1[81]). Of these, 6 proteins were similarly upregulated in NV treatment (CKAP4, LAMP1, GALNT2, NDUFB10, RPL38, RPS19); while 26 proteins may be attributed to HB-EGF function in NV^{HBEGF} (**Figure 4B**).

Erlotinib treatment disrupted phosphorylation of ERBB/EGFR signalling players – a potential mechanism by which NV^{HBEGF} and NVs reprogram HEC1A cells. We analysed the proteome of HEC1A cells following ErloNV^{HBEGF} treatment and compared with NV^{HBEGF} treatment. Indeed, of 127 proteins downregulated (107 absent, 20 significantly downregulated) by ErloNV^{HBEGF} treatment compared to NV^{HBEGF} (**Figure 4C**) included 3 proteins associated with ERBB/EGFR signalling: (i) MTOR, a protein synthesis regulator that forms a positive feedback loop to AKT signalling; (ii) GRB2, upstream regulator of MAPK and PI3K signalling pathways; and (iii) RPS6KA1, a gene expression regulator. Processes associated with the downregulated proteins include vesicle-mediated transport, symbiotic process, organelle organisation, and cellular localisation; with 86 proteins categorised as 'KW-0597: phosphoprotein' (**Figure 4C, Table 6**). Indeed, the phosphorylation expression levels of their 13 associated kinases were decreased following ErloNV^{HBEGF} treatment compared to NV^{HBEGF}, including AKT1, CDK1/9/16, CHEK1, CSNK1A1, IKBKB, LIMK1, MAPK1, MET, PRKCD, RPS6KA1, SRC (**Figure 4D**).

To correlate how cellular changes are altered in HEC1A cells by NV^{HBEGF} and its influence on the endometrium at the time of implantation, we identified upregulated and downregulated proteins in NV^{HBEGF} compared to ErloNV^{HBEGF} and vehicle (**Figure 4E**). We note that compared to NV^{HBEGF}, ErloNV^{HBEGF} treatment downregulated players involved downstream of the EGFR signalling pathway (MAPK1/3/14, BCAR1, IQGAP1, CRKL, INPPL1, CAV1, AP2A1, CAMK2G, GSK3B, PLCG2, NRAS), highlighting EGFR signalling as a central mechanism of NV^{HBEGF}-mediated endometrial reprogramming. Interestingly, proteins upregulated by NV^{HBEGF} have been shown to be also upregulated in expression at the embryo-maternal interface[68, 70] (GSTO1, FKBP1A, ISG15, MAP2K1, AHCYL2,

SWAP70, PPP1CB, LAMA3, RPS20, RPL14). In this study, these identified differentially expressed proteins are involved in symbiotic process, membrane trafficking, and intracellular localisation and transport (**Figure 4F, Table S7**). Contrastingly, processes relating to metabolism (nitrogen, carbon, small molecule) and RNA splicing and biogenesis were associated with ErloNV^{HBEGF} and PBS treatment respectively (**Figure 4F, Table S8/9**).

Collectively, we highlight the capacity of NV-mediated reprogramming of endometrial cells to modulate proteome dynamics associated with EGFR signalling and changes in the endometrium associated with embryo attachment. We next questioned whether HB-EGF-loaded NVs from human trophectodermal cells could regulate endometrial function. Our data suggests that HB-EGF-loaded NVs potentially display the capacity to enhance cell attachment/adhesion and invasive capacity, as previously reported in trophectodermal cell-derived NVs and secreted EVs. This hypothesis was tested.

3.5. NV^{HBEGF} treatment significantly enhances endometrial-trophectoderm adhesion following uptake by recipient endometrial cells

Using a co-culture attachment assay as an *in vitro* proxy measure of adhesive capacity[82, 83], we assessed whether NV^{HBEGF} treatment onto HEC1A cells enhances their adhesion to trophectodermal spheroids (**Figure 5A**). Low-receptive HEC1A endometrial cells (monolayer) were stimulated with treatments for 24 hrs, then incubated with hTSC spheroids and allowed 2 hrs for attachment. Unattached spheroids were removed, remaining attached spheroids were counted, and the attachment rate assessed (**Figure 5A**). NV^{HBEGF} treatment demonstrated the highest significant increase in spheroid attachment rate to HEC1A cells (%) at 65±10 – almost 40% higher than PBS control (27±6, $p<0.005$) (**Figure 5B**) and 20% higher than NVs (46±7, $p<0.005$). However, in ErloNV^{HBEGF} (21±6, $p<0.005$), NV^{HBEGF} did not restore the attachment capabilities of spheroids pre-treated with Erlotinib (to PBS levels); lastly, HB-EGF treatment alone performed similarly to unloaded NVs (42±25, $p>0.05$) (**Figure 5B**).

3.6. NV^{HBEGF} treatment with trophectodermal spheroids significantly enhances their invasive capacity into Matrigel™ matrix

Trophoblast invasion and outgrowth into the endometrium is a hallmark of successful implantation and placentation[73, 84-86] and assessed *in vitro* using the Matrigel™ matrix invasion assay[39, 45, 83] (**Figure 5C**). Here, trophectodermal spheroids were incubated with corresponding treatments for 2 hrs prior to seeding into Matrigel™. A second dose of treatment in media was supplemented after 24 hrs and the level of invasion monitored across 72 hrs using light microscopy (**Figure 5E, F**). Increase in invasion was measured by subtracting the area of the original spheroid from the final measured area of invasion

(**Figure 5E, F**). NV^{HBEGF} treatment displayed the highest significant increase in spheroid invasion (%) at 248.7±75.1 – approximately 1.5-times higher than PBS (185±32.6, $p<0.0005$), while NV (237.9±76.9, $p>0.05$) and HB-EGF (210.5±79.5, $p<0.05$) treatment performed similarly (**Figure 5D**). From our observations with $ErloNV^{HBEGF}$ (80.9±36.4, $p<0.0005$), EGFR inhibition with erlotinib diminished the invasive capacity of spheroids which could not be restored by subsequent NV^{HBEGF} treatment (**Figure 5D**).

Our findings demonstrate the enhanced functional impact of HB-EGF loading into NVs by demonstrating increased (i) attachment of low receptive endometrial cells to trophectodermal spheroids and (ii) invasion of trophectodermal spheroids into Matrigel™ matrix, compared to unmodified NVs. In doing so, we highlight EGFR signalling as a critical mediator of NV^{HBEGF} function.

Discussion

Nanosized extracellular vesicles and a plethora of growth factors (i.e., HB-EGF) are critical signalling mediators during embryo implantation to the maternal endometrium – a cardinal event of pregnancy establishment. This study highlights a rapid and scalable cell extrusion method to load the implantation regulator HB-EGF into trophectodermal cell-derived nanovesicles (NV^{HBEGF}). Our study employs phosphoproteomics and proteomics analysis to demonstrate NV^{HBEGF} short-term signalling and long-term reprogramming capabilities on recipient low receptive HEC1A human endometrial cells. We highlight that NV^{HBEGF} elicit EGFR-mediated effects in recipient endometrial cells. Importantly, these protein phosphorylation activities and signalling patterns, including the activation of kinases and phosphorylation sites that regulate their function (i.e., AKT1 S124[64] and S129[65], MAPK1 T185 and Y187[66]); and signalling processes (i.e., AKT signal transduction, GTPase activity) downstream of EGFR activation; induce functional changes in recipient cells to enhance endometrial attachment to the trophectoderm, and trophectodermal invasion into Matrigel™ matrix.

At the implantation site, trophectodermal cells of the blastocyst release EVs enriched with bioactive molecules that reprogram itself[87-91] and the endometrium[16-18, 92] to support embryo-maternal crosstalk and implantation. NVs derived from hTSCs[17] therefore retain a high proportion of bioactive proteins innate to trophectodermal cells, including those implicated in embryo-maternal interactions (ANXA2[93-95], DPP4[96, 97], CTSB[98-100]) and trophoblast invasion (TAGLN2[73], CTSB/D[99], LGALS3[85]). Indeed, we show that hTSC NV^{HBEGF} and NVs, enriched in these molecules, are effective supplements for promoting endometrial adhesion to trophectodermal cells and trophectodermal invasion into Matrigel™ (**Figure 5**). Similarly in various applications, NV composition can be tailored to suit various therapeutic purposes, such as the selection of macrophages for spinal cord[27] or tumour[20] targeting, stem cells for their regenerative properties[22, 23, 28], and insulin-producing cells for diabetes management[101].

However, the parental cells' natural composition can often limit their function, requiring dose titrations and functional assays[15, 102] to determine an effective dose, although selection of the appropriate functional assays and their standardisation remains an area of active discussion[15].

Modifying NV composition is a method of fine-tuning their function; for example loading of chemotherapeutic drugs[20, 103] for cancer therapy or drug-specific investigations, or antioxidative enzymes[24, 104] for oxidative stress-related diseases; it may thus be explored further to achieve a range of outcomes in different contexts. The extrusion strategy described in this study, for example, can be amended to load other factors to enhance implantation, such as those explored in clinical trials (i.e., hCG (NCT01786252[105], NCT01030393[106])), without genetically modifying parental hTSCs[107]. While HB-EGF was selected for enrichment into NVs for its indispensable roles in pregnancy establishment[30-33, 36, 108-111], its well-researched mechanism of action makes it a suitable target for functional validation and for dissecting the embryo-maternal interface. HB-EGF interacts with receptor tyrosine kinases (RTKs) EGFR and ERBB4 expressed on target cells to initiate multiple downstream signalling cascades[35, 112] (i.e., MAPK, PI3K-AKT/PIP, small GTPase) (reviewed[113]). Furthermore, HB-EGF may perform synergistically with the high expression of heparan sulfate proteoglycans[114] expressed in NVs from their trophectodermal source, as this enhances their binding to high-affinity receptors (i.e., ERBB4[109]), potentially augmenting its influence in recipient cells. However, given the variety of signalling patterns initiated by EGFR, this can induce variable phenotypic responses and outcomes in cells[115-118]; for example, GTPase activity regulates cytoskeletal remodelling and cell polarity[119, 120] in endometrial cells to enhance their adhesive capacity[93, 121, 122]; in embryos, however, it influences transcription activity and signalling (CREB, WNT, JNK)[123, 124] to modulate cell differentiation[124] and embryo size[123]. We have thus assessed the temporal effects of NV^{HBEGF} treatment; from the early phosphorylation-mediated signalling events occurring in recipient cells, to its molecular landscape and function at the approximate time of embryo attachment (1 to 2 days[69]).

The proteome of recipient HEC1A endometrial cells indicates expression of 5 other RTKs (AXL, DDR1, MET, MST1R, EPHA2), which may interact with corresponding ligands enriched in NVs (i.e., LGALS3, collagens, HGF) to activate signalling cascades that converge with the EGFR-mediated pathway[125]. For example, proteins phosphorylated by NV^{HBEGF} and NVs (i.e., GAB1, NCK2, and AKT1), while categorised as EGFR signalling players, are also contributors of MAPK, PI3K-AKT, and MTOR signalling – all present downstream of RTK activation[126]. Indeed, upon EGFR inhibition, subsequent NV^{HBEGF} treatment induced EPHA2 phosphorylation and downstream signalling modulators (i.e., BRAF, MAP3K2, PAK4, PXN, SH3KBP1) (**Figure 3B**). NV^{HBEGF} may also activate cell-surface receptor CD44[55] expressed on HEC1A endometrial cells, which interaction with HB-EGF[56, 127] was previously implicated in endometrial tissue remodelling[55]. CD44 is integral for endometrial decidualisation[127] and adhesion to the embryo[128]; with its expression linked to implantation

success[127] and female fertility status[129]. Upon binding to compatible ligands, CD44 phosphorylates GAB1[130] to initiate AKT signalling, and activates downstream effectors including RhoGTPases[131-133], to induce cytoskeletal reorganisation and cell migration and adhesion. Interestingly, despite EGFR inhibition, NV^{HBEGF} induced the phosphorylation of GAB1 (S163) (**Figure 3B**), and other proteins implicated in the regulation of GTPase activity, supporting NV^{HBEGF}-CD44 interaction as another pivotal driver of endometrial reprogramming. At the site of embryo implantation, GTPase activity exerts influence on PI3K-AKT signalling and RhoA in mouse embryos to mediate their implantation[134], endometrial cell contraction/migration[120, 135], and focal adhesion[119, 135-137]; it is thus an indispensable mediator of embryo-endometrial interactions[93, 121, 122]. Compared to endometrial cells, hTSCs and their derived EVs were enriched in GTPases[17]; the latter's treatment onto recipient endometrial cells upregulated cytoskeletal organisation and cell polarity processes, potentially through GTPase activity as a trophectoderm-mediated signalling strategy. Indeed, supplementation of our unloaded NVs significantly augmented the adhesive capacity of HEC1A endometrial cells to trophectodermal spheroids, as well as the invasive capacity of trophectodermal cells (**Figure 5**). Whether the latter observation is attributed to PI3K-AKT signalling[134] still warrants investigation.

We have demonstrated marked functional influence of NV^{HBEGF} on HEC1A endometrial cells compared to HB-EGF and NVs; which significantly augmented their adhesion to trophectoderm cells by ~40% from baseline (PBS) – double the capacity of HB-EGF and NVs (**Figure 5**). Given that NV^{HBEGF} and HB-EGF share a higher proportion of upregulated proteins in endometrial cells compared to NVs, and the well-studied role of HB-EGF[30-33, 36, 108-111] and ERBB/EGFR[116, 138-140] signalling at the embryo-maternal interface, we posit that the latter has substantial influence on our functional observations. Indeed, with the erlotinib targeted inhibition of EGFR[141], NV^{HBEGF} treatment could not restore endometrial or trophectodermal cell function to baseline (PBS) levels. Moreover, amongst the phosphorylation of kinases and expression of their corresponding proteins downregulated by EGFR inhibition (**Figure 4D**), the most dysregulated proteins include those upregulated at implantation sites[70, 142] (**Figure 4E**). Even so, the functional capacity of HB-EGF was inconsistent, and at best comparable to NVs; a similar phenomenon was observed in hCG-loaded EVs from human uterine fluid[143], which demonstrated the enhanced capacity to induce expression of receptivity markers in recipient endometrial cells compared to hCG alone, EVs alone, or co-supplementation of hCG with EVs. Prior attempts to develop signalling mediators (i.e., hCG[9], LIF[10], and G-CSF[13]) with strong links to fertility and endometrial receptivity as fertility-enhancing supplements have also been unsuccessful in clinical trials. Taken together, these observations allude to a multi-faceted signalling mechanism by engineered EVs or NVs that encompass properties of their enriched molecule and their biological source, thereby enhancing their functional benefit and potential therapeutic utility. NVs thus represent a feasible and adaptable method of large-scale generation of therapeutic vesicles for tuning endometrial phenotype and function. This proof-of-concept study demonstrate feasibility in enhancing the potency of NVs in

the context of embryo attachment and pregnancy establishment. Whether these loaded NVs improve implantation rate *in vivo* warrants future investigation.

Supporting Information

Supporting information is available from the Wiley Online Library or from the author.

Acknowledgements

The authors acknowledge T3-TSC cells were a generous gift from Prof. Susan Fisher (University of California, San Francisco). We thank Bio21 Molecular Science and Biotechnology Institute for assisting with cryo-electron microscopy (University of Melbourne), and Monique Fatmous for editorial assistance. This work was supported by fellowships from Amelia Hains and Baker Institute (DWG) and the National Heart Foundation of Australia (DWG: Vanguard), Aust. National Health and Medical Research Council Project (DWG: #1057741), Future Fund (DWG: MRF1201805), Pankind Aust. (DWG), and the Victorian Government's Operational Infrastructure Support Program. QHP is supported by a joint Baker Institute-La Trobe University Research Training Program Scholarship.

Author Contributions

QHP, AR, and DWG conceived and designed experiments. QHP carried out majority of experiments. JC assisted with proteomic sample preparation. QHP, AR, and DWG wrote, reviewed, and edited the manuscript. All authors approved the final manuscript.

Conflicts of interest: The authors declare no competing interests.

Data and Software Availability: All mass spectrometry data and spectral identifications have been deposited in the ProteomeXchange Consortium via the MASSive partner repository with the identifier MSV000092562 (NV composition, reprogrammed cell phosphoproteomics, reprogrammed cell global proteomics).

Figure Legends

Figure 1. Production and characterisation of NV^{HBEGF}. A) NV^{HBEGF} were generated by serial extrusion (10, 5, 1 μm filters, 13 times per membrane) of human trophectodermal cells (T3-TSCs) with either 50 ng/ml of HB-EGF or PBS and purified using density-cushion ultracentrifugation to obtain 7 fractions (F1-7) of increasing density. NV-containing fraction (F5) was obtained. B) Cryo-electron microscopic image of NV^{HBEGF} displayed spherical and morphologically intact structures; scale 100 nm. C) Size distribution of NV^{HBEGF} based on cryo-electron microscopic images (n=4) reveal enrichment of particles 50-150 nm in diameter. D) Abundance of HB-EGF using mass spectrometry analysis; normalised LFQ intensities (log_2) of HB-EGF between NV^{HBEGF} and NVs generated using the same workflow from hTSCs and mouse embryonic fibroblasts. E) Western blot display of HB-EGF enrichment in NV^{HBEGF} compared to NVs (n=3).

Figure 2. Uptake of NV^{HBEGF} and NVs by HEC1A endometrial cells

A) Confocal fluorescent microscopy images demonstrating uptake of NV^{HBEGF} or NVs labelled with DiI lipophilic fluorescent dye labelled (red) by HEC1A endometrial cells after a 2-h incubation (n=3). B) Fluorescent Z-stack image displaying intracellular distribution of DiI-labelled NV^{HBEGF} (red). Nuclei of HEC1A endometrial cells were stained with Hoechst (blue). Scale bar 10 μm.

Figure 3. NV^{HBEGF} remodel the phosphoproteome landscape in HEC1A endometrial cells. A) Workflow for NV^{HBEGF} and NV treatment onto recipient HEC1A endometrial cells, including a 2-step treatment of erlotinib (EGFR inhibition) followed by NV^{HBEGF} stimulation, and subsequent cell phosphoproteome preparation and analysis. B) Heatmap expression (log_2) of phosphorylated proteins and phosphosites of players of the EGFR signalling pathway, which are downregulated when EGFR is inhibited by erlotinib (white corresponds to missing values). C) (Top) Erlotinib inhibited the phosphorylation of 421 proteins (compared to PBS), while subsequent NV^{HBEGF} treatment induced phosphorylation of 261 of the inhibited proteins; (Bottom) bubble plot displaying key biological processes and pathways corresponding to the 421 and 261 proteins respectively.

Figure 4. NV^{HBEGF} remodel the proteome landscape and EGFR signaling network at the time of implantation. A) Workflow employed for proteomic analysis of stimulated HEC1A endometrial cells. B) Proteins uniquely identified and significantly upregulated in NV^{HBEGF}- or NV-treated HEC1A cells compared to PBS. C) Pre-treatment of HEC1A cells with erlotinib followed by NV^{HBEGF} downregulated the expression of 127 proteins compared to NV^{HBEGF}, which are categorised into related biological processes. D) NV^{HBEGF}- and $ErloNV^{HBEGF}$–mediated phosphorylation levels of 13 kinases that are matched to downregulated proteins. E) Comparative analysis of HEC1A cellular proteome treated with NV^{HBEGF} compared to $ErloNV^{HBEGF}$ and PBS, and a two-way scatter plot highlighting top dysregulated

proteins in the presence of EGFR inhibitor, erlotinib. F) Bubble plot display of biological processes and pathways associated with proteins significantly upregulated (including unique) by NV^{HBEGF} treatment and proteins significantly downregulated (including absent) in NV^{HBEGF} compared to $ErloNV^{HBEGF}$ and PBS.

Figure 5. NV^{HBEGF} enhances attachment to endometrial cells and outgrowth and invasion in Matrigel™ of trophectodermal spheroids. A) Experimental workflow for co-culture attachment assay. B) Box plot indicating percentage of spheroid attachment to HEC1A endometrial cells following treatment with PBS, NV^{HBEGF}, NV, HB-EGF, or $ErloNV^{HBEGF}$ (n=5), where rate of spheroid attachment (%) is the number of attached spheroids divided by the number of seeded spheroids expressed as a percentage. C) Experimental workflow for TSC spheroid outgrowth and invasion into Matrigel™. D) Box plot indicating quantified area of TSC spheroid outgrowth and invasion into Matrigel™ 72 hr following treatment with PBS, NV^{HBEGF}, NV, HB-EGF, or $ErloNV^{HBEGF}$ (n=8). E) Bright-field microscopic images of TSC spheroids outgrowth and invasion into Matrigel™ 72 hr following treatment with PBS, NV^{HBEGF}, NV, HB-EGF, or $ErloNV^{HBEGF}$. Scale bar 100 µm. F) Area of outgrowth extending from spheroid taken for measurements is shaded in grey and quantified using ImageJ. *p<0.05, **p<0.005, ***p<0.0005, ****p<0.001

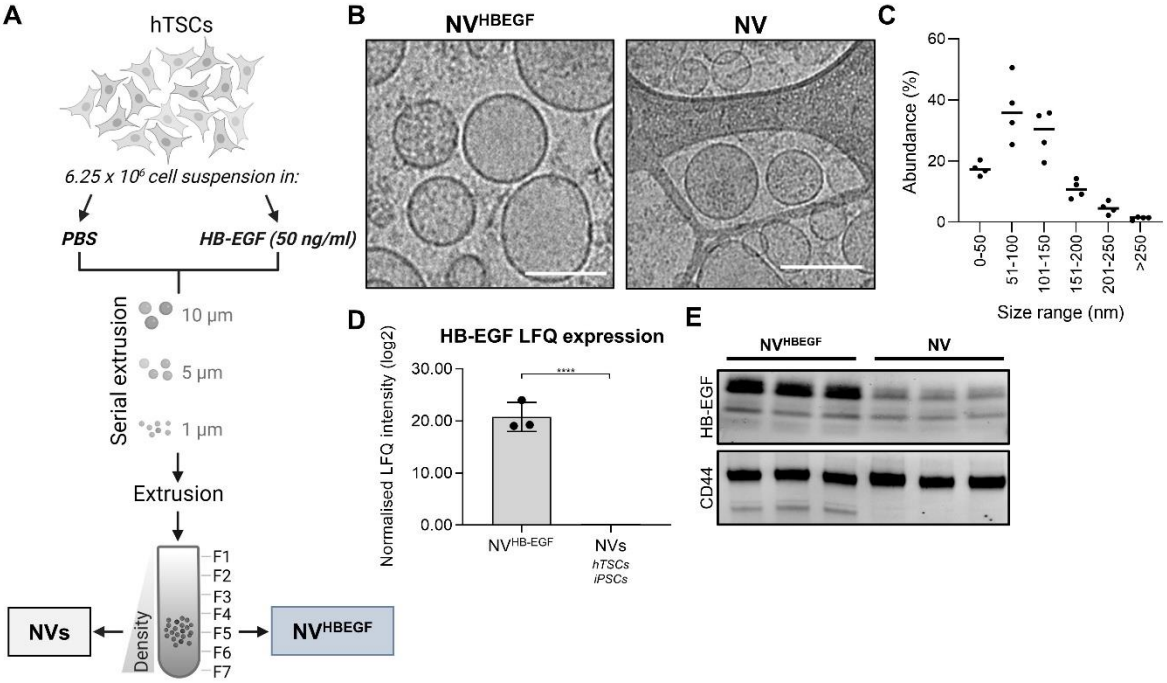

Figure 1. Production and characterisation of $NV^{HB\text{-}EGF}$

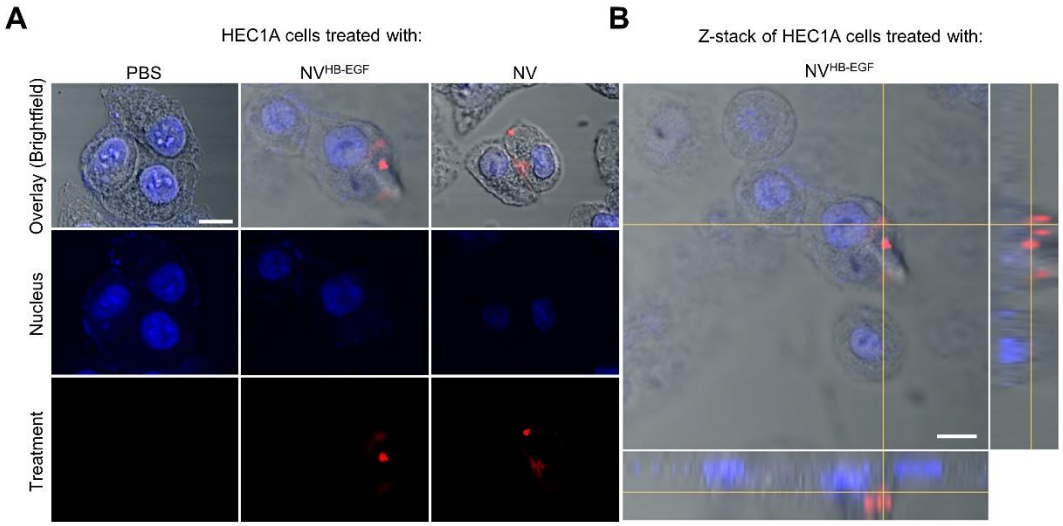

Figure 2. Uptake of $NV^{HB\text{-}EGF}$ and NVs by endometrial HEC1A cells

627
628

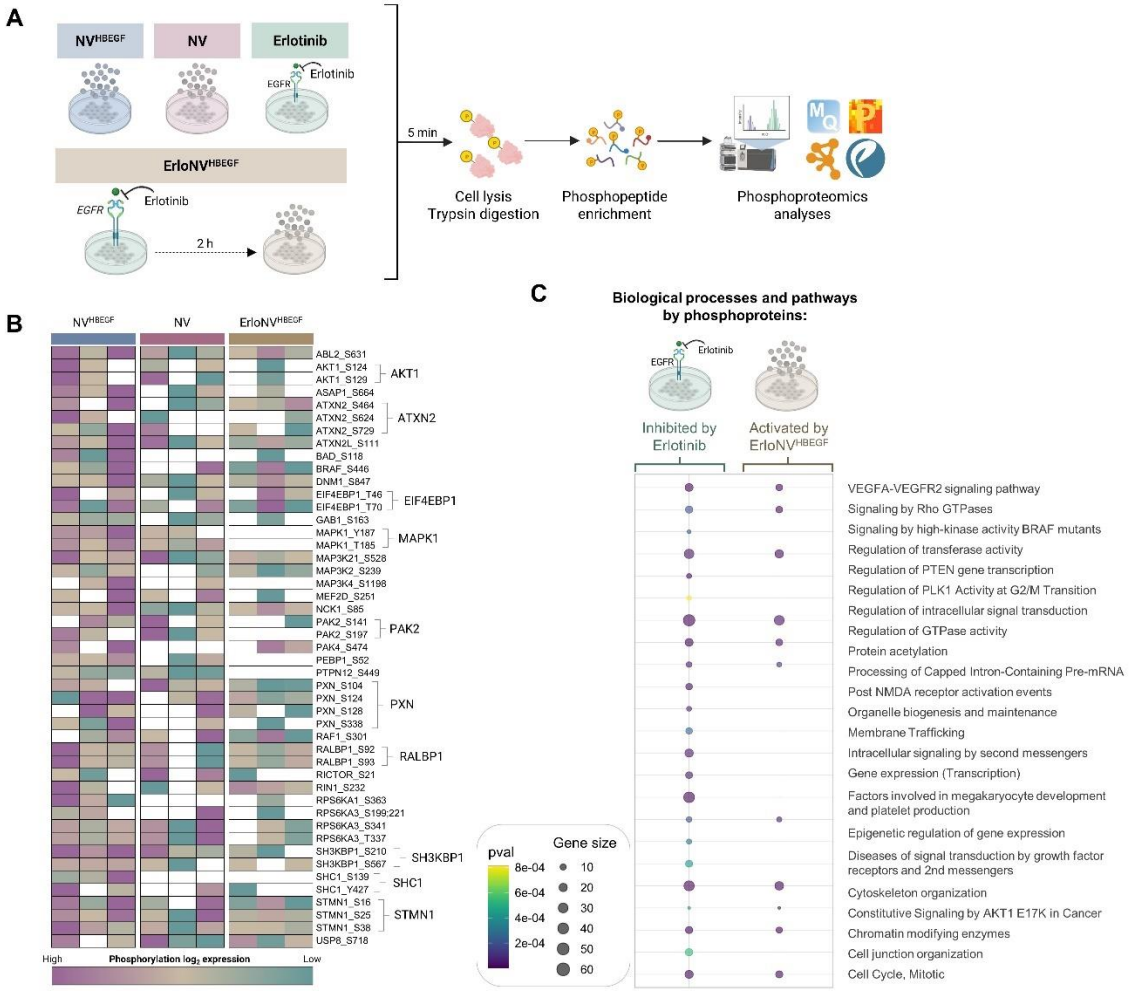

Figure 3. NV^{HBEGF} remodel the phosphoproteome landscape in HEC1A endometrial cells

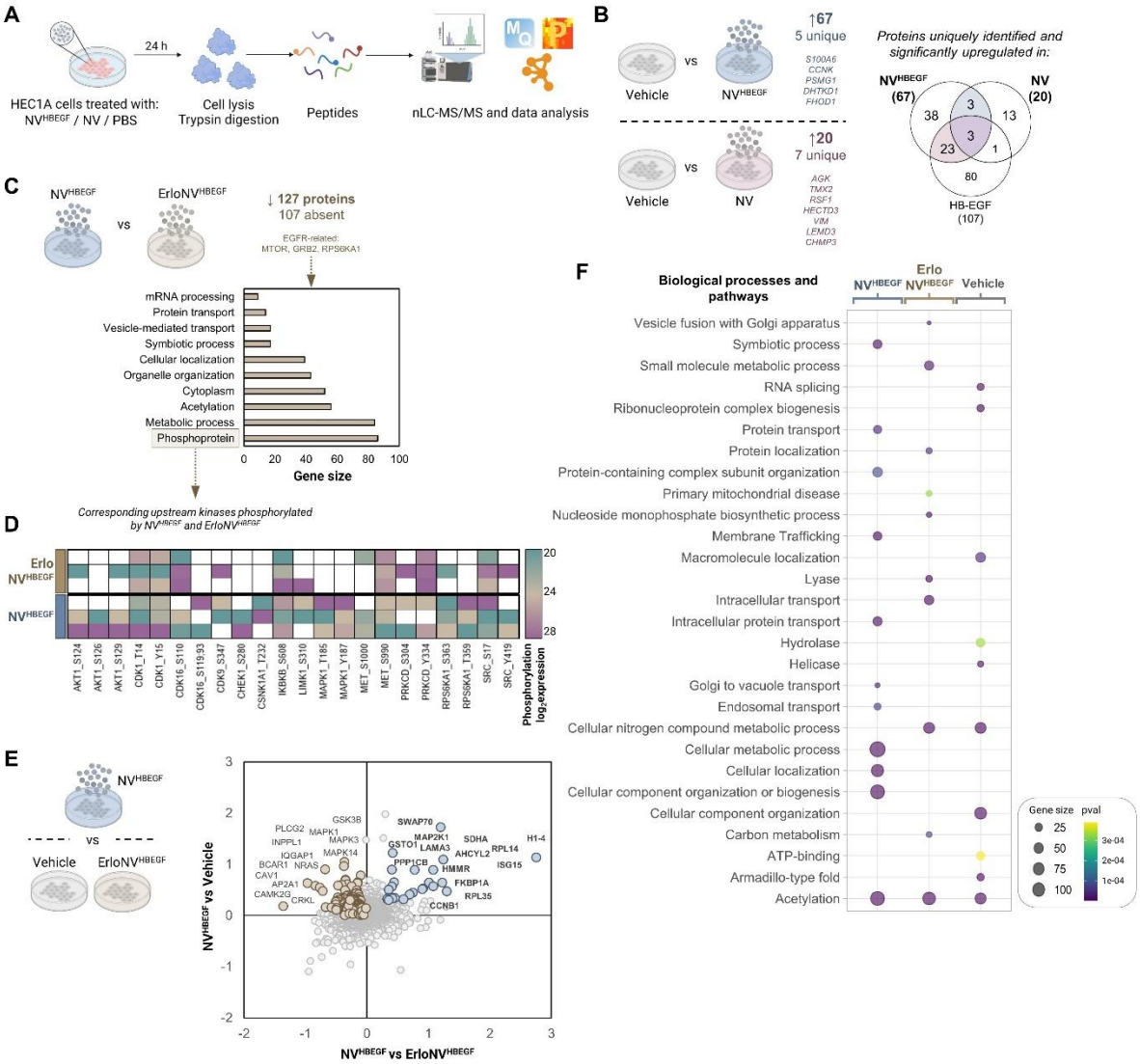

Figure 4. NV^HBEGF remodel the proteome landscape and EGFR signaling network at the time of implantation

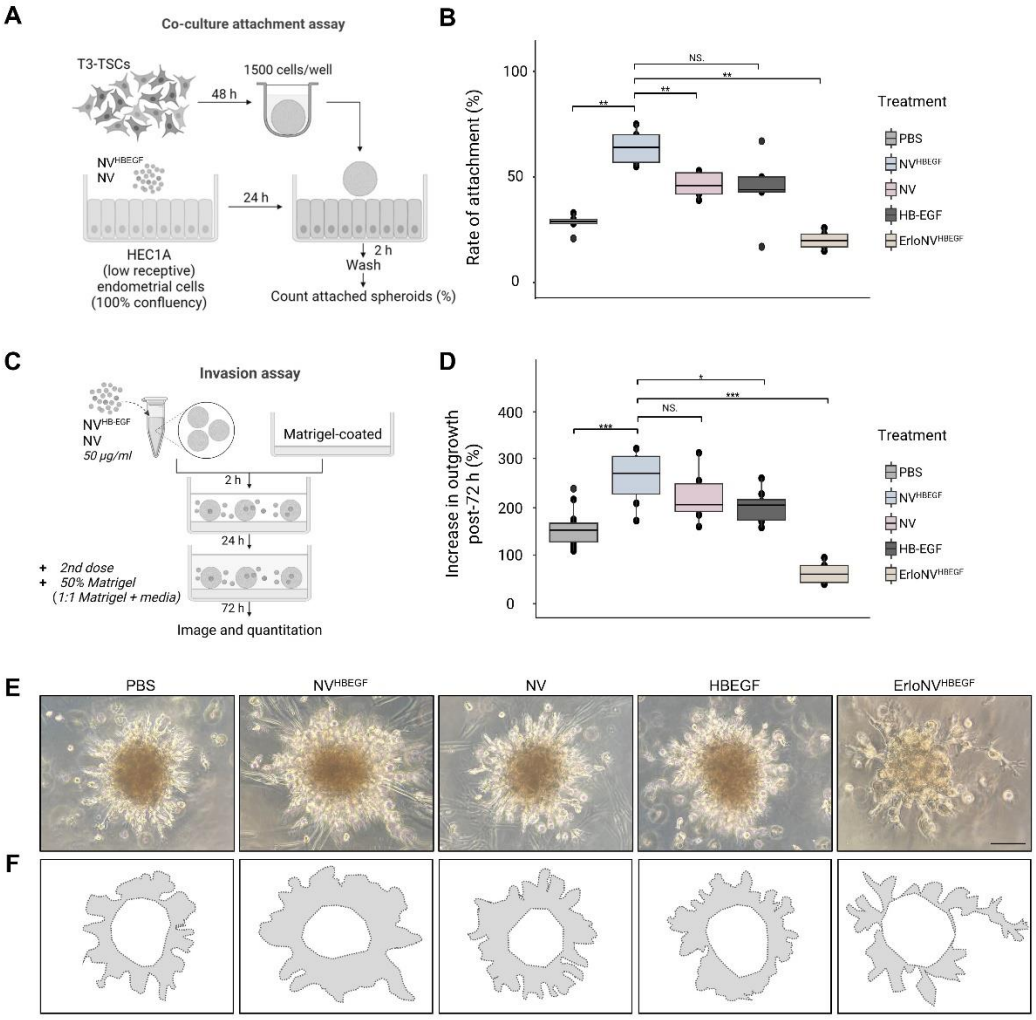

Figure 5. NV$^{HB\text{-}EGF}$ enhances attachment to endometrial cells and outgrowth and invasion in Matrigel of trophectodermal spheroids.

631

References

[1] Wilcox, A. J., Weinberg, C. R., O'Connor, J. F., Baird, D. D.*, et al.*, Incidence of Early Loss of Pregnancy. *The New England Journal of Medicine* 1988, *319*, 189-194.

[2] Zinaman, M. J., Clegg, E. D., Brown, C. C., O'Connor, J., Selevan, S. G., Estimates of human fertility and pregnancy loss. *Fertility and Sterility* 1996, *65*, 503-509.

[3] Macklon, N. S., Geraedts, J. P., Fauser, B. C., Conception to ongoing pregnancy: the 'black box' of early pregnancy loss. *Hum Reprod Update* 2002, *8*, 333-343.

[4] Liu, D., Chen, Y., Ren, Y., Yuan, P.*, et al.*, Primary specification of blastocyst trophectoderm by scRNA-seq: New insights into embryo implantation. *Sci Adv* 2022, *8*, eabj3725.

[5] Wang, W., Vilella, F., Alama, P., Moreno, I.*, et al.*, Single-cell transcriptomic atlas of the human endometrium during the menstrual cycle. *Nature Medicine* 2020, *26*, 1644-1653.

[6] Rosenbluth, E. M., Shelton, D. N., Wells, L. M., Sparks, A. E. T., Van Voorhis, B. J., Human embryos secrete microRNAs into culture media - a potential biomarker for implantation. *Fertility and Sterility* 2014, *101*, 1493-1500.

[7] Cuman, C., Van Sinderen, M., Gantier, M. P., Rainczuk, K.*, et al.*, Human Blastocyst Secreted microRNA Regulate Endometrial Epithelial Cell Adhesion. *EBioMedicine* 2015, *2*, 1528-1535.

[8] Kaneko, Y., Murphy, C. R., Day, M. L., Extracellular matrix proteins secreted from both the endometrium and the embryo are required for attachment: a study using a co-culture model of rat blastocysts and Ishikawa cells. *J Morphol* 2013, *274*, 63-72.

[9] Craciunas, L., Tsampras, N., Raine-Fenning, N., Coomarasamy, A., Intrauterine administration of human chorionic gonadotropin (hCG) for subfertile women undergoing assisted reproduction. *Cochrane Database Syst Rev* 2018, *10*, CD011537.

[10] Brinsden, P. R., Alam, V., de Moustier, B., Engrand, P., Recombinant human leukemia inhibitory factor does not improve implantation and pregnancy outcomes after assisted reproductive techniques in women with recurrent unexplained implantation failure. *Fertil Steril* 2009, *91*, 1445-1447.

[11] Ledee-Bataille, N., Olivennes, F., Kadoch, J., Dubanchet, S.*, et al.*, Detectable levels of interleukin-18 in uterine luminal secretions at oocyte retrieval predict failure of the embryo transfer. *Hum Reprod* 2004, *19*, 1968-1973.

[12] Rodriguez-Wallberg, K. A., Munding, B., Ziebe, S., Robertson, S. A., GM-CSF does not rescue poor-quality embryos: secondary analysis of a randomized controlled trial. *Arch Gynecol Obstet* 2020, *301*, 1341-1346.

[13] Kalem, Z., Namli Kalem, M., Bakirarar, B., Kent, E.*, et al.*, Intrauterine G-CSF Administration in Recurrent Implantation Failure (RIF): An Rct. *Sci Rep* 2020, *10*, 5139.

[14] Greening, D. W., Xu, R., Ale, A., Hagemeyer, C. E., Chen, W., Extracellular Vesicles as Next Generation Immunotherapeutics. *Semin Cancer Biol* 2023.

[15] Claridge, B., Lozano, J., Poh, Q. H., Greening, D. W., Development of Extracellular Vesicle Therapeutics: Challenges, Considerations, and Opportunities. *Front Cell Dev Biol* 2021, *9*, 734720.

[16] Su, Y., Li, Q., Zhang, Q., Li, Z.*, et al.*, Exosomes derived from placental trophoblast cells regulate endometrial epithelial receptivity in dairy cows during pregnancy. *J Reprod Dev* 2022, *68*, 21-29.

[17] Poh, Q. H., Rai, A., Carmichael, II, Salamonsen, L. A., Greening, D. W., Proteome reprogramming of endometrial epithelial cells by human trophectodermal small extracellular vesicles reveals key insights into embryo implantation. *Proteomics* 2021, *21*, e2000210.

[18] Godakumara, K., Ord, J., Lattekivi, F., Dissanayake, K.*, et al.*, Trophoblast derived extracellular vesicles specifically alter the transcriptome of endometrial cells and may constitute a critical component of embryo-maternal communication. *Reprod Biol Endocrinol* 2021, *19*, 115.

[19] Gurung, S., Greening, D. W., Catt, S., Salamonsen, L., Evans, J., Exosomes and soluble secretome from hormone-treated endometrial epithelial cells direct embryo implantation. *Mol Hum Reprod* 2020, *26*, 510-520.

[20] Jang, S. C., Kim, O. Y., Yoon, C. M., Choi, D. S.*, et al.*, Bioinspired exosome-mimetic nanovesicles for targeted delivery of chemotherapeutics to malignant tumors. *ACS Nano* 2013, *7*, 7698-7710.
[21] Nasiri Kenari, A., Kastaniegaard, K., Greening, D. W., Shambrook, M.*, et al.*, Proteomic and Post-Translational Modification Profiling of Exosome-Mimetic Nanovesicles Compared to Exosomes. *Proteomics* 2019, *19*, e1800161.
[22] Wang, X., Hu, S., Li, J., Zhu, D.*, et al.*, Extruded Mesenchymal Stem Cell Nanovesicles Are Equally Potent to Natural Extracellular Vesicles in Cardiac Repair. *ACS Appl Mater Interfaces* 2021, *13*, 55767-55779.
[23] Lee, H., Cha, H., Park, J. H., Derivation of Cell-Engineered Nanovesicles from Human Induced Pluripotent Stem Cells and Their Protective Effect on the Senescence of Dermal Fibroblasts. *Int J Mol Sci* 2020, *21*.
[24] Haney, M. J., Klyachko, N. L., Zhao, Y., Gupta, R.*, et al.*, Exosomes as drug delivery vehicles for Parkinson's disease therapy. *J Control Release* 2015, *207*, 18-30.
[25] Hajipour, H., Sambrani, R., Ghorbani, M., Mirzamohammadi, Z., Nouri, M., Sildenafil citrate-loaded targeted nanostructured lipid carrier enhances receptivity potential of endometrial cells via LIF and VEGF upregulation. *Naunyn Schmiedebergs Arch Pharmacol* 2021, *394*, 2323-2331.
[26] Aleksejeva, E., Zarovni, N., Dissanayake, K., Godakumara, K.*, et al.*, Extracellular vesicle research in reproductive science: Paving the way for clinical achievements†. *Biology of Reproduction* 2021, *106*, 408-424.
[27] Lee, J. R., Kyung, J. W., Kumar, H., Kwon, S. P.*, et al.*, Targeted Delivery of Mesenchymal Stem Cell-Derived Nanovesicles for Spinal Cord Injury Treatment. *Int J Mol Sci* 2020, *21*, 4185.
[28] Lozano, J., Rai, A., Lees, J. G., Fang, H.*, et al.*, Scalable Generation of Nanovesicles from Human-Induced Pluripotent Stem Cells for Cardiac Repair. *Int J Mol Sci* 2022, *23*.
[29] Paria, B. C., Ma, W., Tan, J., Raja, S.*, et al.*, Cellular and molecular responses of the uterus to embryo implantation can be elicited by locally applied growth factors. *Proc Natl Acad Sci U S A* 2001, *98*, 1047-1052.
[30] Das, S. K., Wang, X. N., Paria, B. C., Damm, D.*, et al.*, Heparin-binding EGF-like growth factor gene is induced in the mouse uterus temporally by the blastocyst solely at the site of its apposition: a possible ligand for interaction with blastocyst EGF-receptor in implantation. *Development* 1994, *120*, 1071-1083.
[31] Lim, H. J., Dey, S. K., HB-EGF: a unique mediator of embryo-uterine interactions during implantation. *Exp Cell Res* 2009, *315*, 619-626.
[32] Lim, J. J., Lee, D. R., Song, H.-S., Kim, K.-S.*, et al.*, Heparin-binding epidermal growth factor (HB-EGF) may improve embryonic development and implantation by increasing vitronectin receptor (integrin alphanubeta3) expression in peri-implantation mouse embryos. *Journal of assisted reproduction and genetics* 2006, *23*, 111-119.
[33] Leach, R. E., Khalifa, R., Ramirez, N. D., Das, S. K.*, et al.*, Multiple roles for heparin-binding epidermal growth factor-like growth factor are suggested by its cell-specific expression during the human endometrial cycle and early placentation. *J Clin Endocrinol Metab* 1999, *84*, 3355-3363.
[34] Thouas, G. A., Dominguez, F., Green, M. P., Vilella, F.*, et al.*, Soluble Ligands and Their Receptors in Human Embryo Development and Implantation. *Endocrine Reviews* 2015, *36*, 92-130.
[35] Reynolds, C. M., Eguchi, S., Frank, G. D., Motley, E. D., Signaling mechanisms of heparin-binding epidermal growth factor-like growth factor in vascular smooth muscle cells. *Hypertension* 2002, *39*, 525-529.
[36] Jessmon, P., Kilburn, B. A., Romero, R., Leach, R. E., Armant, D. R., Function-specific intracellular signaling pathways downstream of heparin-binding EGF-like growth factor utilized by human trophoblasts. *Biol Reprod* 2010, *82*, 921-929.
[37] Makieva, S., Giacomini, E., Ottolina, J., Sanchez, A. M.*, et al.*, Inside the Endometrial Cell Signaling Subway: Mind the Gap(s). *Int J Mol Sci* 2018, *19*.

[38] Zdravkovic, T., Nazor, K. L., Larocque, N., Gormley, M.*, et al.*, Human stem cells from single blastomeres reveal pathways of embryonic or trophoblast fate specification. *Development* 2015, *142*, 4010-4025.
[39] Evans, J., Rai, A., Nguyen, H. P. T., Poh, Q. H.*, et al.*, Human Endometrial Extracellular Vesicles Functionally Prepare Human Trophectoderm Model for Implantation: Understanding Bidirectional Maternal-Embryo Communication. *Proteomics* 2019, *19*, e1800423.
[40] Evans, J., Walker, K. J., Bilandzic, M., Kinnear, S., Salamonsen, L. A., A novel "embryo-endometrial" adhesion model can potentially predict "receptive" or "non-receptive" endometrium. *J Assist Reprod Genet* 2020, *37*, 5-16.
[41] Liang, J., Li, K., Chen, K., Liang, J.*, et al.*, Regulation of ARHGAP19 in the endometrial epithelium: a possible role in the establishment of uterine receptivity. *Reprod Biol Endocrinol* 2021, *19*, 2.
[42] Vergaro, P., Tiscornia, G., Rodríguez, A., Santaló, J., Vassena, R., Transcriptomic analysis of the interaction of choriocarcinoma spheroids with receptive vs. non-receptive endometrial epithelium cell lines: an in vitro model for human implantation. *J Assist Reprod Genet* 2019, *36*, 857-873.
[43] Tamm, K., Rõõm, M., Salumets, A., Metsis, M., Genes targeted by the estrogen and progesterone receptors in the human endometrial cell lines HEC1A and RL95-2. *Reprod Biol Endocrinol* 2009, *7*, 150.
[44] John, N. J., Linke, M., Denker, H. W., Quantitation of human choriocarcinoma spheroid attachment to uterine epithelial cell monolayers. *In Vitro Cell Dev Biol Anim* 1993, *29A*, 461-468.
[45] Fatmous, M., Rai, A., Poh, Q. H., Salamonsen, L. A., Greening, D. W., Endometrial small extracellular vesicles regulate human trophectodermal cell invasion by reprogramming the phosphoproteome landscape. *Front Cell Dev Biol* 2022, *10*, 1078096.
[46] Claridge, B., Rai, A., Fang, H., Matsumoto, A.*, et al.*, Proteome characterisation of extracellular vesicles isolated from heart. *Proteomics* 2021, *21*, e2100026.
[47] Greening, D. W., Nguyen, H. P., Elgass, K., Simpson, R. J., Salamonsen, L. A., Human Endometrial Exosomes Contain Hormone-Specific Cargo Modulating Trophoblast Adhesive Capacity: Insights into Endometrial-Embryo Interactions. *Biol Reprod* 2016, *94*, 38.
[48] Rai, A., Fang, H., Fatmous, M., Claridge, B.*, et al.*, A Protocol for Isolation, Purification, Characterization, and Functional Dissection of Exosomes. *Methods Mol Biol* 2021, *2261*, 105-149.
[49] Hughes, C. S., Moggridge, S., Muller, T., Sorensen, P. H.*, et al.*, Single-pot, solid-phase-enhanced sample preparation for proteomics experiments. *Nat Protoc* 2019, *14*, 68-85.
[50] Kompa, A. R., Greening, D. W., Kong, A. M., McMillan, P. J.*, et al.*, Sustained subcutaneous delivery of secretome of human cardiac stem cells promotes cardiac repair following myocardial infarction. *Cardiovasc Res* 2020.
[51] Cox, J., Neuhauser, N., Michalski, A., Scheltema, R. A.*, et al.*, Andromeda: a peptide search engine integrated into the MaxQuant environment. *J Proteome Res* 2011, *10*, 1794-1805.
[52] Rai, A., Greening, D. W., Chen, M., Xu, R.*, et al.*, Exosomes Derived from Human Primary and Metastatic Colorectal Cancer Cells Contribute to Functional Heterogeneity of Activated Fibroblasts by Reprogramming Their Proteome. *PROTEOMICS* 2019, *19*, 1800148.
[53] Shannon, P., Markiel, A., Ozier, O., Baliga, N. S.*, et al.*, Cytoscape: a software environment for integrated models of biomolecular interaction networks. *Genome Res* 2003, *13*, 2498-2504.
[54] Hnasko, R., Ben-Jonathan, N., Prolactin regulation by heparin-binding growth factors expressed in mouse pituitary cell lines. *Endocrine* 2003, *20*, 35-44.
[55] Yu, W. H., Woessner, J. F., Jr., McNeish, J. D., Stamenkovic, I., CD44 anchors the assembly of matrilysin/MMP-7 with heparin-binding epidermal growth factor precursor and ErbB4 and regulates female reproductive organ remodeling. *Genes Dev* 2002, *16*, 307-323.
[56] Bennett, K. L., Jackson, D. G., Simon, J. C., Tanczos, E.*, et al.*, CD44 isoforms containing exon V3 are responsible for the presentation of heparin-binding growth factor. *J Cell Biol* 1995, *128*, 687-698.

[57] Chobotova, K., Karpovich, N., Carver, J., Manek, S.*, et al.*, Heparin-binding epidermal growth factor and its receptors mediate decidualization and potentiate survival of human endometrial stromal cells. *J Clin Endocrinol Metab* 2005, *90*, 913-919.
[58] Hornbeck, P. V., Zhang, B., Murray, B., Kornhauser, J. M.*, et al.*, PhosphoSitePlus, 2014: mutations, PTMs and recalibrations. *Nucleic Acids Res* 2015, *43*, D512-520.
[59] Salazar-Cavazos, E., Nitta, C. F., Mitra, E. D., Wilson, B. S.*, et al.*, Multisite EGFR phosphorylation is regulated by adaptor protein abundances and dimer lifetimes. *Mol Biol Cell* 2020, *31*, 695-708.
[60] Liu, N., Matsumoto, M., Kitagawa, K., Kotake, Y.*, et al.*, Chk1 phosphorylates the tumour suppressor Mig-6, regulating the activation of EGF signalling. *EMBO J* 2012, *31*, 2365-2377.
[61] Imami, K., Sugiyama, N., Imamura, H., Wakabayashi, M.*, et al.*, Temporal profiling of lapatinib-suppressed phosphorylation signals in EGFR/HER2 pathways. *Mol Cell Proteomics* 2012, *11*, 1741-1757.
[62] Dibble, C. C., Asara, J. M., Manning, B. D., Characterization of Rictor phosphorylation sites reveals direct regulation of mTOR complex 2 by S6K1. *Mol Cell Biol* 2009, *29*, 5657-5670.
[63] Pan, C., Olsen, J. V., Daub, H., Mann, M., Global effects of kinase inhibitors on signaling networks revealed by quantitative phosphoproteomics. *Mol Cell Proteomics* 2009, *8*, 2796-2808.
[64] Bellacosa, A., Chan, T. O., Ahmed, N. N., Datta, K.*, et al.*, Akt activation by growth factors is a multiple-step process: the role of the PH domain. *Oncogene* 1998, *17*, 313-325.
[65] Di Maira, G., Salvi, M., Arrigoni, G., Marin, O.*, et al.*, Protein kinase CK2 phosphorylates and upregulates Akt/PKB. *Cell Death Differ* 2005, *12*, 668-677.
[66] Bi, J., Koivisto, L., Dai, J., Zhuang, D.*, et al.*, Epidermal growth factor receptor signaling suppresses alphavbeta6 integrin and promotes periodontal inflammation and bone loss. *J Cell Sci* 2019, *133*.
[67] Diaz-Gimeno, P., Horcajadas, J. A., Martinez-Conejero, J. A., Esteban, F. J.*, et al.*, A genomic diagnostic tool for human endometrial receptivity based on the transcriptomic signature. *Fertil Steril* 2011, *95*, 50-60, 60 e51-15.
[68] Wang, F., Zhao, S., Deng, D., Wang, W.*, et al.*, Integrating LCM-Based Spatio-Temporal Transcriptomics Uncovers Conceptus and Endometrial Luminal Epithelium Communication that Coordinates the Conceptus Attachment in Pigs. *Int J Mol Sci* 2021, *22*.
[69] Kim, S. M., Kim, J. S., A Review of Mechanisms of Implantation. *Dev Reprod* 2017, *21*, 351-359.
[70] Aikawa, S., Hirota, Y., Fukui, Y., Ishizawa, C.*, et al.*, A gene network of uterine luminal epithelium organizes mouse blastocyst implantation. *Reprod Med Biol* 2022, *21*, e12435.
[71] Klein, C., Novel equine conceptus?endometrial interactions on Day 16 of pregnancy based on RNA sequencing. *Reprod Fertil Dev* 2015.
[72] Liang, X., Jin, Y., Wang, H., Meng, X.*, et al.*, Transgelin 2 is required for embryo implantation by promoting actin polymerization. *Faseb j* 2019, *33*, 5667-5675.
[73] Wang, H., Zhang, X., Liu, C., Chen, S.*, et al.*, TAGLN2-Regulated Trophoblast Migration, Invasion and Fusion are Impaired in Preeclampsia. *Frontiers in Cell and Developmental Biology* 2022, *10*.
[74] Li, X.-j., Zhao, Z.-a., Gao, L., Regulation and Expression of Tagln2 in Early Rabbit Pregnant Uterus. *Journal of Reproduction and Contraception* 2010, *21*, 27-34.
[75] Haouzi, D., Dechaud, H., Assou, S., Monzo, C.*, et al.*, Transcriptome analysis reveals dialogues between human trophectoderm and endometrial cells during the implantation period. *Hum Reprod* 2011, *26*, 1440-1449.
[76] Lu, L., Chen, Y., Yang, Z., Liang, S.*, et al.*, Expression and Regulation of a Novel Decidual Cells-Derived Estrogen Target during Decidualization. *Int J Mol Sci* 2022, *24*.
[77] Yang, X., Ding, Y., Sun, L., Shi, M.*, et al.*, Ferritin light chain deficiency-induced ferroptosis is involved in preeclampsia pathophysiology by disturbing uterine spiral artery remodelling. *Redox Biol* 2022, *58*, 102555.
[78] Nakashima, A., Cheng, S. B., Kusabiraki, T., Motomura, K.*, et al.*, Endoplasmic reticulum stress disrupts lysosomal homeostasis and induces blockade of autophagic flux in human trophoblasts. *Sci Rep* 2019, *9*, 11466.

[79] Menkhorst, E. M., Lane, N., Winship, A. L., Li, P.*, et al.*, Decidual-secreted factors alter invasive trophoblast membrane and secreted proteins implying a role for decidual cell regulation of placentation. *PLoS One* 2012, *7*, e31418.
[80] Nakashima, A., Cheng, S. B., Ikawa, M., Yoshimori, T.*, et al.*, Evidence for lysosomal biogenesis proteome defect and impaired autophagy in preeclampsia. *Autophagy* 2020, *16*, 1771-1785.
[81] Moore, S. G., McCabe, M. S., Green, J. C., Newsom, E. M., Lucy, M. C., The transcriptome of the endometrium and placenta is associated with pregnancy development but not lactation status in dairy cows. *Biol Reprod* 2017, *97*, 18-31.
[82] Evans, J., Hutchison, J., Salamonsen, L. A., Greening, D. W., Proteomic Insights into Endometrial Receptivity and Embryo-Endometrial Epithelium Interaction for Implantation Reveal Critical Determinants of Fertility. *Proteomics* 2020, *20*, e1900250.
[83] Rai, A., Poh, Q. H., Fatmous, M., Fang, H.*, et al.*, Proteomic profiling of human uterine extracellular vesicles reveal dynamic regulation of key players of embryo implantation and fertility during menstrual cycle. *Proteomics* 2021, *21*, e2000211.
[84] Liu, C., Yao, W., Yao, J., Li, L.*, et al.*, Endometrial extracellular vesicles from women with recurrent implantation failure attenuate the growth and invasion of embryos. *Fertil Steril* 2020, *114*, 416-425.
[85] Bojic-Trbojevic, Z., Jovanovic Krivokuca, M., Vilotic, A., Kolundzic, N.*, et al.*, Human trophoblast requires galectin-3 for cell migration and invasion. *Sci Rep* 2019, *9*, 2136.
[86] Gardner, D. K., Lactate production by the mammalian blastocyst: manipulating the microenvironment for uterine implantation and invasion? *Bioessays* 2015, *37*, 364-371.
[87] Desrochers, L. M., Bordeleau, F., Reinhart-King, C. A., Cerione, R. A., Antonyak, M. A., Microvesicles provide a mechanism for intercellular communication by embryonic stem cells during embryo implantation. *Nature Communications* 2016.
[88] Qu, P., Qing, S., Liu, R., Qin, H.*, et al.*, Effects of embryo-derived exosomes on the development of bovine cloned embryos. *PLoS One* 2017, *12*, e0174535.
[89] Pavani, K. C., Meese, T., Pascottini, O. B., Guan, X.*, et al.*, Hatching is modulated by microRNA-378a-3p derived from extracellular vesicles secreted by blastocysts. *Proceedings of the National Academy of Sciences* 2022, *119*, e2122708119.
[90] Kim, J., Lee, J., Lee, T. B., Jun, J. H., Embryotrophic effects of extracellular vesicles derived from outgrowth embryos in pre- and peri-implantation embryonic development in mice. *Mol Reprod Dev* 2019, *86*, 187-196.
[91] Saadeldin, I. M., Kim, S. J., Choi, Y. B., Lee, B. C., Improvement of Cloned Embryos Development by Co-Culturing with Parthenotes: A Possible Role of Exosomes/Microvesicles for Embryos Paracrine Communication. *Cellular Reprogramming* 2014, *16*.
[92] Es-Haghi, M., Godakumara, K., Haling, A., Lattekivi, F.*, et al.*, Specific trophoblast transcripts transferred by extracellular vesicles affect gene expression in endometrial epithelial cells and may have a role in embryo-maternal crosstalk. *Cell Commun Signal* 2019, *17*, 146.
[93] Garrido-Gómez, T., Dominguez, F., Quiñonero, A., Estella, C.*, et al.*, Annexin A2 is critical for embryo adhesiveness to the human endometrium by RhoA activation through F-actin regulation. *Faseb j* 2012, *26*, 3715-3727.
[94] Wang, B., Shao, Y., Annexin A2 acts as an adherent molecule under the regulation of steroids during embryo implantation. *Mol Hum Reprod* 2020, *26*, 825-836.
[95] Wang, B., Ye, T.-M., Lee, K.-F., Chiu, P. C. N.*, et al.*, Annexin A2 Acts as an Adhesion Molecule on the Endometrial Epithelium during Implantation in Mice. *PloS one* 2015, *10*, e0139506-e0139506.
[96] Dolanbay, E. G., Yardimoglu, M., Yalcinkaya, E., Yazir, Y.*, et al.*, Expression of trophinin and dipeptidyl peptidase IV in endometrial co-culture in the presence of an embryo: A comparative immunocytochemical study. *Mol Med Rep* 2016, *13*, 3961-3968.
[97] Shimomura, Y., Ando, H., Furugori, K., Kajiyama, H.*, et al.*, Possible involvement of crosstalk cell-adhesion mechanism by endometrial CD26/dipeptidyl peptidase IV and embryonal fibronectin in human blastocyst implantation. *Mol Hum Reprod* 2006, *12*, 491-495.

[98] Afonso, S., Romagnano, L., Babiarz, B., The expression and function of cystatin C and cathepsin B and cathepsin L during mouse embryo implantation and placentation. *Development* 1997, *124*, 3415-3425.
[99] Amarante-Paffaro, A. M., Hoshida, M. S., Yokota, S., Goncalves, C. R.*, et al.*, Localization of cathepsins D and B at the maternal-fetal interface and the invasiveness of the trophoblast during the postimplantation period in the mouse. *Cells Tissues Organs* 2011, *193*, 417-425.
[100] Song, G., Bailey, D. W., Dunlap, K. A., Burghardt, R. C.*, et al.*, Cathepsin B, cathepsin L, and cystatin C in the porcine uterus and placenta: potential roles in endometrial/placental remodeling and in fluid-phase transport of proteins secreted by uterine epithelia across placental areolae. *Biol Reprod* 2010, *82*, 854-864.
[101] Oh, K., Kim, S. R., Kim, D. K., Seo, M. W.*, et al.*, In Vivo Differentiation of Therapeutic Insulin-Producing Cells from Bone Marrow Cells via Extracellular Vesicle-Mimetic Nanovesicles. *ACS Nano* 2015, *9*, 11718-11727.
[102] Otero-Ortega, L., Laso-Garcia, F., Frutos, M. C. G., Diekhorst, L.*, et al.*, Low dose of extracellular vesicles identified that promote recovery after ischemic stroke. *Stem Cell Res Ther* 2020, *11*, 70.
[103] Haney, M. J., Zhao, Y., Jin, Y. S., Li, S. M.*, et al.*, Macrophage-Derived Extracellular Vesicles as Drug Delivery Systems for Triple Negative Breast Cancer (TNBC) Therapy. *J Neuroimmune Pharmacol* 2020, *15*, 487-500.
[104] Haney, M. J., Klyachko, N. L., Harrison, E. B., Zhao, Y.*, et al.*, TPP1 Delivery to Lysosomes with Extracellular Vesicles and their Enhanced Brain Distribution in the Animal Model of Batten Disease. *Adv Healthc Mater* 2019, *8*, e1801271.
[105] Strug, M. R., Su, R., Young, J. E., Dodds, W. G.*, et al.*, Intrauterine human chorionic gonadotropin infusion in oocyte donors promotes endometrial synchrony and induction of early decidual markers for stromal survival: a randomized clinical trial. *Hum Reprod* 2016, *31*, 1552-1561.
[106] Mansour, R., Tawab, N., Kamal, O., El-Faissal, Y.*, et al.*, Intrauterine injection of human chorionic gonadotropin before embryo transfer significantly improves the implantation and pregnancy rates in in vitro fertilization/intracytoplasmic sperm injection: a prospective randomized study. *Fertil Steril* 2011, *96*, 1370-1374 e1371.
[107] Wang, B., Yao, K., Huuskes, B. M., Shen, H. H.*, et al.*, Mesenchymal Stem Cells Deliver Exogenous MicroRNA-let7c via Exosomes to Attenuate Renal Fibrosis. *Mol Ther* 2016, *24*, 1290-1301.
[108] Martin, K. L., Barlow, D. H., Sargent, I. L., Heparin-binding epidermal growth factor significantly improves human blastocyst development and hatching in serum-free medium. *Hum Reprod* 1998, *13*, 1645-1652.
[109] Paria, B. C., Elenius, K., Klagsbrun, M., Dey, S. K., Heparin-binding EGF-like growth factor interacts with mouse blastocysts independently of ErbB1: a possible role for heparan sulfate proteoglycans and ErbB4 in blastocyst implantation. *Development* 1999, *126*, 1997-2005.
[110] Xie, H., Wang, H., Tranguch, S., Iwamoto, R.*, et al.*, Maternal heparin-binding-EGF deficiency limits pregnancy success in mice. *Proc Natl Acad Sci U S A* 2007, *104*, 18315-18320.
[111] Liu, Z., Armant, D. R., Lysophosphatidic acid regulates murine blastocyst development by transactivation of receptors for heparin-binding EGF-like growth factor. *Exp Cell Res* 2004, *296*, 317-326.
[112] Jin, K., Mao, X. O., Del Rio Guerra, G., Jin, L., Greenberg, D. A., Heparin-binding epidermal growth factor-like growth factor stimulates cell proliferation in cerebral cortical cultures through phosphatidylinositol 3'-kinase and mitogen-activated protein kinase. *J Neurosci Res* 2005, *81*, 497-505.
[113] Oda, K., Matsuoka, Y., Funahashi, A., Kitano, H., A comprehensive pathway map of epidermal growth factor receptor signaling. *Mol Syst Biol* 2005, *1*, 2005 0010.
[114] Higashiyama, S., Abraham, J. A., Klagsbrun, M., Heparin-binding EGF-like growth factor stimulation of smooth muscle cell migration: dependence on interactions with cell surface heparan sulfate. *J Cell Biol* 1993, *122*, 933-940.

[115] Speth, Z., Islam, T., Banerjee, K., Resat, H., EGFR signaling pathways are wired differently in normal 184A1L5 human mammary epithelial and MDA-MB-231 breast cancer cells. *J Cell Commun Signal* 2017, *11*, 341-356.
[116] Large, M. J., Wetendorf, M., Lanz, R. B., Hartig, S. M.*, et al.*, The epidermal growth factor receptor critically regulates endometrial function during early pregnancy. *PLoS Genet* 2014, *10*, e1004451.
[117] Kohei, M., Fusanori, Y., Sung Ouk, N. A. M., Masahide, K., Shingo, M., Regulatory Mechanisms of the HB-EGF Autocrine Loop in Inflammation, Homeostasis, Development and Cancer. *Anticancer Research* 2012, *32*, 2347.
[118] Chen, J., Zeng, F., Forrester, S. J., Eguchi, S.*, et al.*, Expression and Function of the Epidermal Growth Factor Receptor in Physiology and Disease. *Physiol Rev* 2016, *96*, 1025-1069.
[119] Cox, E. A., Sastry, S. K., Huttenlocher, A., Integrin-mediated adhesion regulates cell polarity and membrane protrusion through the Rho family of GTPases. *Mol Biol Cell* 2001, *12*, 265-277.
[120] Rottner, K., Hall, A., Small, J. V., Interplay between Rac and Rho in the control of substrate contact dynamics. *Curr Biol* 1999, *9*, 640-648.
[121] Heneweer, C., Kruse, L. H., Kindhauser, F., Schmidt, M.*, et al.*, Adhesiveness of human uterine epithelial RL95-2 cells to trophoblast: rho protein regulation. *Mol Hum Reprod* 2002, *8*, 1014-1022.
[122] Heneweer, C., Schmidt, M., Denker, H.-W., Thie, M., Molecular mechanisms in uterine epithelium during trophoblast binding: the role of small GTPase RhoA in human uterine Ishikawa cells. *Journal of Experimental & Clinical Assisted Reproduction* 2005, *2*, 4.
[123] Sordella, R., Classon, M., Hu, K. Q., Matheson, S. F.*, et al.*, Modulation of CREB activity by the Rho GTPase regulates cell and organism size during mouse embryonic development. *Dev Cell* 2002, *2*, 553-565.
[124] Loebel, D. A., Tam, P. P., Rho GTPases in endoderm development and differentiation. *Small GTPases* 2012, *3*, 40-44.
[125] Sudhesh Dev, S., Zainal Abidin, S. A., Farghadani, R., Othman, I., Naidu, R., Receptor Tyrosine Kinases and Their Signaling Pathways as Therapeutic Targets of Curcumin in Cancer. *Front Pharmacol* 2021, *12*, 772510.
[126] Mendoza, M. C., Er, E. E., Blenis, J., The Ras-ERK and PI3K-mTOR pathways: cross-talk and compensation. *Trends Biochem Sci* 2011, *36*, 320-328.
[127] Zhou, X., Cao, Y., Zhou, M., Han, M.*, et al.*, Decreased CD44v3 expression impairs endometrial stromal cell proliferation and decidualization in women with recurrent implantation failure. *Reprod Biol Endocrinol* 2022, *20*, 170.
[128] Berneau, S. C., Ruane, P. T., Brison, D. R., Kimber, S. J.*, et al.*, Investigating the role of CD44 and hyaluronate in embryo-epithelial interaction using an in vitro model. *Mol Hum Reprod* 2019, *25*, 265-273.
[129] Paravati, R., De Mello, N., Onyido, E. K., Francis, L. W.*, et al.*, Differential regulation of osteopontin and CD44 correlates with infertility status in PCOS patients. *Journal of Molecular Medicine* 2020, *98*, 1713-1725.
[130] Bourguignon, L. Y., Singleton, P. A., Zhu, H., Diedrich, F., Hyaluronan-mediated CD44 interaction with RhoGEF and Rho kinase promotes Grb2-associated binder-1 phosphorylation and phosphatidylinositol 3-kinase signaling leading to cytokine (macrophage-colony stimulating factor) production and breast tumor progression. *J Biol Chem* 2003, *278*, 29420-29434.
[131] Bourguignon, L. Y., Gilad, E., Peyrollier, K., Brightman, A., Swanson, R. A., Hyaluronan-CD44 interaction stimulates Rac1 signaling and PKN gamma kinase activation leading to cytoskeleton function and cell migration in astrocytes. *J Neurochem* 2007, *101*, 1002-1017.
[132] Zhang, Y., Xia, H., Ge, X., Chen, Q.*, et al.*, CD44 acts through RhoA to regulate YAP signaling. *Cell Signal* 2014, *26*, 2504-2513.
[133] Oliferenko, S., Kaverina, I., Small, J. V., Huber, L. A., Hyaluronic acid (HA) binding to CD44 activates Rac1 and induces lamellipodia outgrowth. *J Cell Biol* 2000, *148*, 1159-1164.
[134] Liu, L., Wang, Y., Yu, Q., The PI3K/Akt signaling pathway exerts effects on the implantation of mouse embryos by regulating the expression of RhoA. *Int J Mol Med* 2014, *33*, 1089-1096.

[135] Chrzanowska-Wodnicka, M., Burridge, K., Rho-stimulated contractility drives the formation of stress fibers and focal adhesions. *J Cell Biol* 1996, *133*, 1403-1415.
[136] Kumar, V., Soni, U. K., Maurya, V. K., Singh, K., Jha, R. K., Integrin beta8 (ITGB8) activates VAV-RAC1 signaling via FAK in the acquisition of endometrial epithelial cell receptivity for blastocyst implantation. *Sci Rep* 2017, *7*, 1885.
[137] Tu, Z., Wang, Q., Cui, T., Wang, J.*, et al.*, Uterine RAC1 via Pak1-ERM signaling directs normal luminal epithelial integrity conducive to on-time embryo implantation in mice. *Cell Death & Differentiation* 2016, *23*, 169-181.
[138] Large, M. J., Hartig, S. M., Franco, H. L., Kovanci, E.*, et al.*, Demonstrating the Critical Role of Uterine Erbb Signaling in Fertility. *Biology of Reproduction* 2010, *83*, 17-17.
[139] Cai, L., Zhang, J., Duan, E., Dynamic distribution of epidermal growth factor during mouse embryo peri-implantation. *Cytokine* 2003, *23*, 170-178.
[140] Sugihara, K., Sugiyama, D., Byrne, J., Wolf, D. P.*, et al.*, Trophoblast cell activation by trophinin ligation is implicated in human embryo implantation. *Proc Natl Acad Sci U S A* 2007, *104*, 3799-3804.
[141] Nishimura, T., Nakamura, K., Yamashita, S., Ikeda, S.*, et al.*, Effect of the molecular targeted drug, erlotinib, against endometrial cancer expressing high levels of epidermal growth factor receptor. *BMC Cancer* 2015, *15*, 957.
[142] Chen, Y., Ni, H., Ma, X.-H., Hu, S.-J.*, et al.*, Global analysis of differential luminal epithelial gene expression at mouse implantation sites. *Journal of Molecular Endocrinology* 2006, *37*, 147-161.
[143] Hajipour, H., Farzadi, L., Roshangar, L., Latifi, Z.*, et al.*, A human chorionic gonadotropin (hCG) delivery platform using engineered uterine exosomes to improve endometrial receptivity. *Life Sci* 2021, *275*, 119351.